

Supporting information for

Push-Pull [7]Helicene Diimide: Excited-State Charge Transfer and Solvatochromic Circularly Polarized Luminescence

Fridolin Saal,^a Asim Swain,^a Alexander Schmiedel,^a Marco Holzapfel,^a Christoph Lambert,^a and Prince Ravat*^a

^aJulius-Maximilians-Universität Würzburg, Institut für Organische Chemie, Am Hubland, D-97074 Würzburg, Germany.

Table of contents

S1. Experimental Details	2
S2. Synthesis and Materials	5
S3. Optical Spectroscopy	9
S4. Cyclic Voltammetry and Spectroelectrochemistry.....	12
S5. Lippert-Mataga equation.....	13
S6. Chiral stationary phase HPLC	14
S7. Determination of barrier of enantiomerization	15
S8. Quantum Chemical Calculations	16
S9. NMR spectroscopy.....	20
S10. High-resolution mass spectrometry (HRMS)	27
S11. Cartesian Coordinates.....	28
S12. References.....	30

S1. Experimental Details

Chromatography:

Open-column chromatography and thin-layer chromatography (TLC) were performed on silica gel (Merck silica gel 60M, 40–63 μm).

NMR Spectroscopy:

The NMR experiments were performed at 298 K on NMR spectrometers operating at 400 MHz ^1H and 101 MHz ^{13}C frequencies. Standard pulse sequences were used, and the data was processed using 2-fold zero-filling in the indirect dimension for all 2D experiments. Chemical shifts (δ) are reported in parts per million (ppm) relative to the solvent residual peak (^1H and ^{13}C NMR, respectively): CDCl_3 ($\delta = 7.26$ and 77.16 ppm), and J values are given in Hz. Structural assignment was made with additional information from $g\text{COSY}$, $g\text{ROESY}$ and $g\text{NOESY}$ experiments.

HRMS:

MALDI-TOF-HRMS were measured on a Bruker ultrafleXtreme mass spectrometer. *Trans*-2-[3-(4-*tert*-butylphenyl)-2-methyl-2-propenylidene]malononitrile (DCTB) dissolved in chloroform (30mg/mL) was used as supporting matrix in the MALDI-TOF-HRMS measurement.

Melting Point:

Melting points were measured using an OptiMelt automated melting point system from Stanford research systems.

UV-vis Absorption Spectroscopy:

UV-vis spectra were measured on a JASCO V-670 spectrophotometer.

Emission Spectroscopy:

Room temperature fluorescence emission spectra were measured on an Edinburgh FLS 980 photoluminescence spectrometer.

Fluorescence Lifetime and Quantum Yield:

The fluorescence quantum yields were measured on an Edinburgh Instruments FLS980 fluorescence lifetime spectrometer using a 450 W xenon arc lamp as a light source and a calibrated integrating sphere. Fluorescence lifetimes were measured on the same spectrometer using either a 418.6 nm or 378.2 nm pulsed laser diode with a pulse frequency of 1/100 ns. The fluorescence lifetime was determined from a biexponential fit in *n*-hexane and methylcyclohexane and from a monoexponential fit in all other solvents.

Transient Absorption Spectroscopy:

Femtosecond transient absorption spectra of **2** were recorded on a setup consisting of a laser “Solstice” from Newport-Spectra-Physics, an OPA “TOPAS” from Light Conversion, and a spectrometer “Helios” from Ultrafast Systems. The Solstice provides laser pulses with a fundamental wavelength of $12\,500\text{ cm}^{-1}$ (800 nm), a repetition rate of 1 kHz, and a temporal pulse width of 100 fs. A very small part of around 2 μJ is split off for creating the probe white light continuum (WLC). This small part is led over a computer controlled linear stage with a retro reflector to set the time difference between the pump and the probe pulses from 0 fs to 4 ps in 20 fs intervals and from 4 ps to 8 ns in logarithmic steps with a maximum size of 200 ps.

The Helios consists of fibre coupled spectrometers with CMOS sensors which are sensitive from $32\,260\text{ cm}^{-1}$ to $10\,930\text{ cm}^{-1}$ (310 nm to 915 nm) and have an intrinsic resolution of 1.5 nm. The pump beam and the probe light meet at an angle of 6° vertically in the cuvette. By using wire grid polarizers, the polarization axes were set to the magic angle to avoid isotropic effects. The obtained IRF was determined to 100 fs by fitting the rise time.

The WLC is created by using a linear oscillating CaF_2 crystal. To receive the probe, range from 400 nm to 800 nm, a coloured glass filter “BG38” and a dielectric 400 nm steep-edge long pass filter were used. The WLC is split into two parts before the sample to correct intensity fluctuations of the white light generation with a reference channel. The TOPAS was set to the excitation wavelength of $24\,510\text{ cm}^{-1}$ (408 nm) in DCM, $24\,570\text{ cm}^{-1}$ (407 nm) and $26\,110\text{ cm}^{-1}$ (386 nm) in MeCN, and the pulse energy was attenuated with a ND-filter wheel to 30 nJ in DCM, 400 nJ for in MeCN. All measurements were performed in fused silica cuvettes (Starna GmbH) with an optical path length of 1 mm at room temperature. All samples were filtered after dissolution. The optical density was adjusted to around 0.4 at the corresponding excitation wavenumber for DCM and to the solubility limit in MeCN.

Electronic Circular Dichroism and Circularly Polarized Luminescence Spectroscopy:

Electronic Circular Dichroism (ECD) and Circularly Polarized Luminescence (CPL) were recorded with a customized JASCO CPL-300/J-1500 hybrid spectrometer.

Spectroelectrochemistry

Spectroelectrochemical experiments in reflection mode were performed using an Agilent Cary 5000 spectrophotometer in combination with a custom designed sample compartment consisting of a cylindrical PTFE cell with a sapphire window and an adjustable two-in-one electrode (6 mm platinum disc working electrode, 1 mm platinum wire counter electrode). The potentials were adjusted referencing to a silver/silver chloride leak free reference electrode. All experiments were performed at room temperature under an argon atmosphere. The optical path length was adjusted to 0.1 mm and 0.1 M $[\text{Bu}_4\text{N}][\text{PF}_6]$ was used as supporting electrolyte.

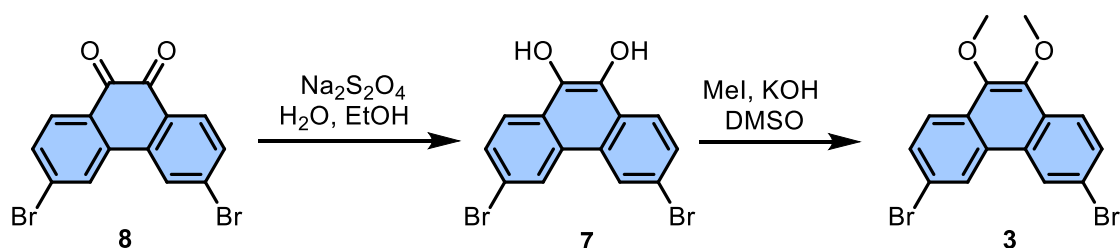
Cyclic voltammetry and Differential Pulse Voltammetry

Cyclic voltammetry and Differential Pulse Voltammetry experiments were performed in THF and acetonitrile with 0.1 M $[\text{Bu}_4\text{N}][\text{PF}_6]$ as supporting electrolyte using a Gamry Instruments Reference 600 potentiostat. A standard three-electrode cell configuration was employed using a platinum disk working electrode, a platinum wire counter electrode, and a platinum wire serving as reference electrode. The redox potentials were referenced to the ferrocene (Fc) / ferrocenium (Fc^+) redox couple.

S2. Synthesis and Materials

All chemicals and solvents were purchased from commercial sources and were used without further purification unless stated otherwise. The reactions and experiments that are sensitive to dioxygen were performed using Schlenk techniques and nitrogen-saturated solvents. Compound **8**¹ and N-(*n*-butyl)-4-homophthalimide² were prepared according to the respective literature.

S2.1 Synthesis of 3,6-dibromo-9,10-dimethoxyphenanthrene (**3**)



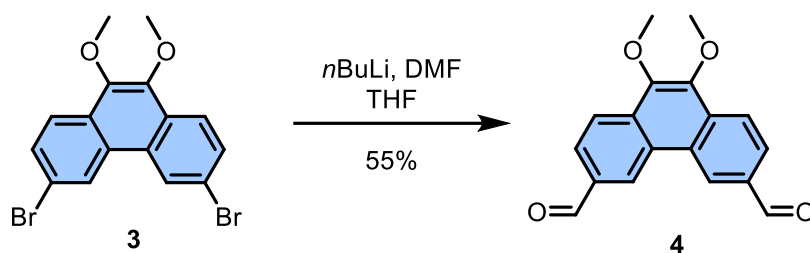
To a nitrogen-saturated solution of sodium dithionite (14.4 g, 82.6 mmol, 4.00 equiv.) in a mixture of THF (150 mL) and water (50 mL), 3,6-Dibromo-9,10-phenanthrene-9,10-dione (**8**, 7.56 g, 20.7 mmol, 1.00 equiv.) was added. The mixture was stirred under N_2 overnight until dissipation of the bright yellow colour. The mixture was extracted with Et_2O (4 x 50 mL), and the combined organic phases were dried over MgSO_4 . The solvents were evaporated, and the off-white residue (crude **7**) was dissolved in DMSO (100 mL) together with potassium hydroxide (4.40 g, 77.8 mmol, 4.00 equiv.). Methyl iodide (12.1 mL, 194 mmol, 10.0 equiv.) was added dropwise at 0 °C. The mixture was stirred overnight at room temperature. The solution was poured into water (100 mL) and neutralized with saturated NH_4Cl solution. The aqueous phase was extracted with DCM (4x 50 mL) and the combined organic phases were dried over MgSO_4 and evaporated under reduced pressure. The bright yellow residue was purified by recrystallization from a mixture 4:1 of EtOH/EtOAc .

Yield: 4.32 g (10.9 mmol, 53 %) of **3** over two steps.

Melting point: 137–139 °C (from EtOH/EtOAc)

¹H NMR (400 MHz, CDCl_3 , rt): δ [ppm] = 8.65 (d, J = 1.9 Hz, 2H), 8.09 (d, J = 8.7 Hz, 2H), 7.72 (dd, J = 8.7, 1.9 Hz, 2H), 4.07 (s, 6H).

S2.2 Synthesis of 9,10-dimethoxyphenanthrene-3,6-dicarbaldehyde (**4**)



3,6-Dibromo-9,10-dimethoxyphenanthrene (**3**) (3.00 g, 7.57 mmol, 1.00 equiv.) was dissolved in THF under inert gas and cooled to $-78\text{ }^{\circ}\text{C}$. A solution of 1.6 M *n*-butyllithium in hexane (10.4 mL, 16.6 mmol, 2.20 equiv.) was added dropwise over 15 minutes and the mixture was stirred for one hour at $-78\text{ }^{\circ}\text{C}$. DMF (5.86 mL, 75.7 mmol, 10.0 equiv.) was added dropwise and stirring was continued for 1 hour more after which the temperature was slowly raised to room temperature and stirring was continued for 2 hours. The reaction mixture was quenched with ammonium chloride solution and poured on 50 mL of water in a separation funnel. The mixture was extracted with DCM (3 x 50 mL) and the combined organic phases were washed with water (2 x 50 mL). The organic solvent was evaporated, and the obtained pale yellow crude product was purified by recrystallization from a mixture of 9:1 toluene/*n*-hexane.

Yield: 1.23 g (4.18 mmol, 55 %)

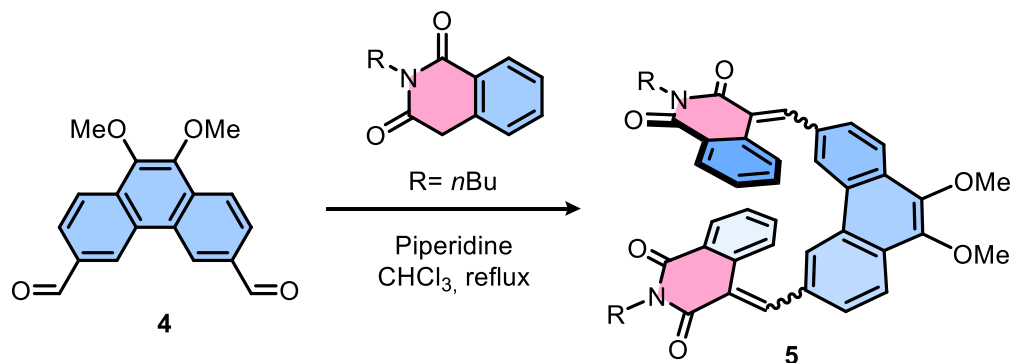
Melting point: 182–188 $^{\circ}\text{C}$ (from toluene/*n*-hexane, slow decomposition)

^1H NMR (400 MHz, CDCl_3 , rt): δ [ppm] = 10.30 (d, $J = 0.6$ Hz, 2H), 9.22 (d, $J = 1.5$ Hz, 2H), 8.45 – 8.39 (m, 2H), 8.16 (dd, $J = 8.5, 1.5$ Hz, 2H), 4.15 (s, 6H).

^{13}C NMR (101 MHz, CDCl_3 , rt): δ [ppm] = 192.2, 146.3, 134.3, 133.8, 128.6, 126.8, 126.4, 123.7, 61.3.

HRMS (MALDI): m/z : calculated $[\text{M}]^+$ 294.08866; found $[\text{M}]^+$ 294.08904 ($|\Delta| = 1.29$ ppm).

S2.3. Synthesis of 4,4'-((9,10-dimethoxyphenanthrene-3,6-diyl)bis(methaneylylidene))bis(2-butylisoquinoline-1,3(2H,4H)-dione) (5)



N-(*n*-butyl)-4-homophthalimide (2.03 g, 7.48 mmol, 2.20 equiv.) and **4** (1.00 g, 3.39 mmol, 1.00 equiv.) were dissolved in chloroform (40 mL) under inert atmosphere. Piperidine (577 mg, 6.78 mmol, 2.00 equiv.) was added and the mixture was refluxed for 15 h. The reaction solution was washed with NH₄Cl solution (20 mL) and water (20 mL) and the organic phase was separated and dried over MgSO₄. The organic layer was evaporated under reduced pressure and the residue was purified by overlaying a saturated solution of the crude product in DCM with twice the amount of MeOH and letting the mixture rest at room temperature for 2 days. This led to formation of needle-shaped crystals of almost exclusively one isomer.

Yield: 1.61 g (2.32 mmol, 69 %).

Melting point: 113–115 °C (from DCM/MeOH)

¹H NMR (400 MHz, CDCl₃, rt): δ [ppm] = 8.58 (s, 2H), 8.35 (s, 2H), 8.28 – 8.24 (m, 2H), 8.22 (d, J = 8.5 Hz, 2H), 7.70 – 7.66 (m, 2H), 7.58 (dt, J = 8.0, 1.0 Hz, 2H), 7.38 (ddd, J = 8.1, 7.3, 1.2 Hz, 2H), 7.16 (ddd, J = 8.1, 7.3, 1.5 Hz, 2H), 4.14 (s, 3H), 4.12 – 4.07 (m, 4H), 1.75 – 1.65 (m, 4H), 1.48 – 1.40 (m, 4H), 0.99 (t, J = 7.3 Hz, 6H).

Since the minor isomers could not completely be removed, no further characterization by NMR was carried out. The purity of the sample was confirmed by HRMS (MALDI, **Fig. S21**).

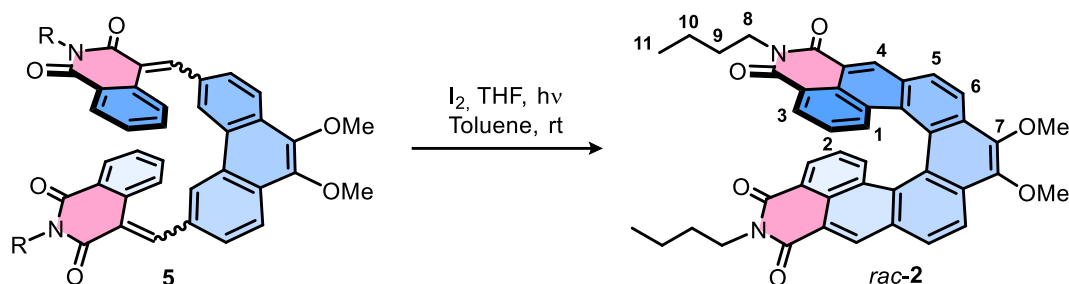
HRMS (MALDI): m/z : calculated [M]⁺ 692.28809; found [M]⁺ 692.28775 ($|\Delta|$ = 0.49 ppm).

S2.4 General conditions for stilbene photocyclodehydrogenation³

Photoreaction apparatus

Photoirradiation was performed with a Heraeus 142 W medium pressure mercury lamp at room temperature. The lamp was encased in a cooling jacket with continuous flow of cooling water. The whole lamp assembly was submerged in a cylindrical photoreaction flask with a volume of either 250 mL or 600 mL. During irradiation, the apparatus was covered in a black box to prevent leakage of radiation.

S2.5. Synthesis of dimethyl-[4,4'-biphenanthrene diimide]-3,3'-dicarboxylate (2)



5 (150 mg, 216 μ mol, 1.00 equiv.) was dissolved in toluene and degassed with nitrogen for 30 minutes. Iodine (121 mg, 476 μ mol, 2.20 equiv.) and THF (3 mL) were added to the mixture, and it was stirred and irradiated until TLC control showed complete consumption of starting material. Residual iodine was quenched with saturated Na₂S₂O₃ solution. The organic phase was separated and dried over MgSO₄ and evaporated under reduced pressure. The residuals were purified by column chromatography on silica gel (PE/EtOAc 75:25) to yield *rac*-**2** as a yellow solid. In accordance with the known preferential formation of helicenes in the Mallory Photocyclization no other isomers of **2** could be isolated.

Yield: 34.2 mg (49.7 μ mol, 23 %).

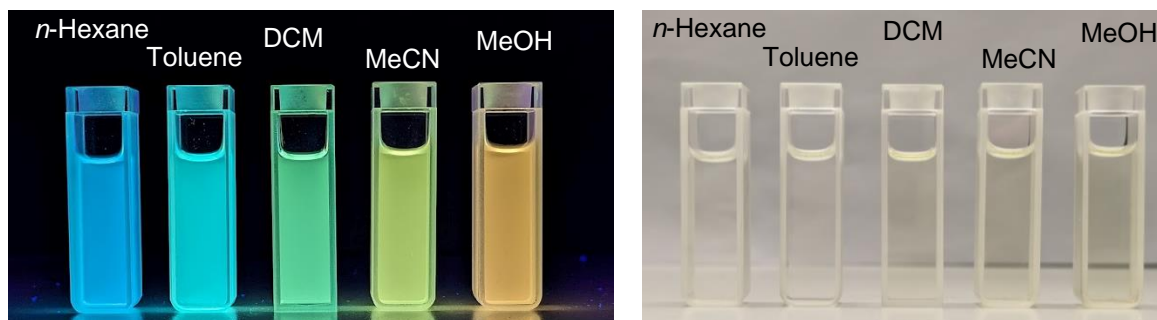
Melting point: >300 °C (decomposition)

¹H NMR (400 MHz, CD₂Cl₂, rt): δ [ppm] = 8.94 (s, 1H, H₄), 8.54 (d, J = 8.5 Hz, 1H, H₆), 8.18 (d, J = 8.6 Hz, 1H, H₅), 7.91 (dd, J = 7.4, 1.1 Hz, 1H, H₃), 7.46 (dd, J = 8.5, 1.1 Hz, 1H, H₁), 6.64 (dd, J = 8.5, 7.4 Hz, 1H, H₂), 4.29 (s, 3H, H₇), 4.14 (t, J = 7.5 Hz, 2H, H₈), 1.70 (td, J = 7.5, 3.7 Hz, 2H, H₉), 1.47 – 1.40 (m, 2H, H₁₀), 1.00 (t, J = 7.4 Hz, 3H, H₁₁).

¹³C NMR (101 MHz, CD₂Cl₂, rt): δ [ppm] = 164.0 (C_q), 163.9 (C_q), 146.0 (C_q), 133.1 (CH), 131.0 (C_q), 130.8 (C_q), 129.9 (C_q), 129.8 (CH), 129.4 (CH), 129.1 (CH), 128.1 (C_q), 126.4 (C_q), 124.9 (CH), 122.7 (C_q), 122.4 (CH), 122.0 (C_q), 120.8 (C_q), 61.6 (CH₃), 40.4 (CH₂), 30.3 (CH₂), 20.5 (CH₂), 14.0 (CH₃).

HRMS (MALDI): m/z : calculated [M]⁺ 688.256788; found [M]⁺ 688.25627 ($|\Delta|$ = 0.75 ppm).

S3. Optical Spectroscopy



Fluorescence of **2** in solvents of increasing polarity (left) and near-uniform light-yellow colour of the same solutions under ambient light (right).

Table S1. Summary of optical properties of **2** in solvents of various polarities.

Solvent	$f(D) - f(n^2)$	$\lambda_{\text{abs}} / \text{nm}$	$\lambda_{\text{em}} / \text{nm}$	$\Delta\nu / \text{cm}^{-1}$	τ / ns	E_g^a / eV	Φ_f	${}^c k_{\text{FL}} / 10^7 \text{ s}^{-1}$	${}^d k_{\text{NR}} / 10^7 \text{ s}^{-1}$	$FWHM / \text{cm}^{-1}$	$g_{\text{abs}} / 10^{-3}$	$g_{\text{lum}} / 10^{-3}$
Hexane	0.00	397	495	4987	5.71 ^b	2.78	0.11	1.93 ^c	15.6 ^c	3221	9.8	4.5
MeCy	0.00	398	500	5126	6.12 ^b	2.76	0.14	2.28 ^c	14.1 ^c	3515	10.1	4.5
Toluene	0.01	405	509	5045	5.97	2.72	0.18	3.01	13.7	3626	11.2	5.0
CHCl ₃	0.15	409	523	5329	5.58	2.67	0.27	4.84	13.2	3583	9.8	4.4
EtOAc	0.20	404	524	5669	6.36	2.70	0.24	3.77	11.9	3855	8.7	4.4
THF	0.21	405	528	5752	7.73	2.69	0.30	3.88	9.06	3840	10.9	4.7
DCM	0.22	408	532	5713	6.01	2.66	0.26	4.33	12.3	3755	8.6	4.2
Acetone	0.28	406	549	6416	7.54	2.66	0.25	3.32	9.95	4003	9.1	4.4
MeCN	0.31	408	554	6459	8.05	2.63	0.25	3.11	9.32	3979	9.5	4.4
DMSO	0.26	414	579	6883	9.31	2.60	0.34	3.65	7.09	4185	8.9	4.2
MeOH	0.31	410	591	7470	4.73	2.57	0.10	2.11	19.0	4184	8.0	2.6

^a Optical energy gap estimated from the crossing of absorption and fluorescence spectra. ^b $\tau_{\text{avg}} = (\alpha_1 \tau_1^2 + \alpha_2 \tau_2^2) / (\alpha_1 \tau_1 + \alpha_2 \tau_2)$ (Ref.⁴). ^c Rate constant for the radiative decay $k_{\text{FL}} = \Phi_{\text{FL}} / \tau_{\text{FL}}$.

^d Rate constant for the non-radiative decay $k_{\text{NR}} = (1 - \Phi_{\text{FL}}) / \tau_{\text{FL}}$.

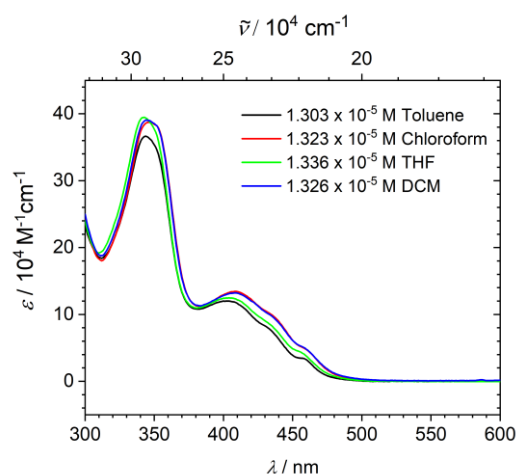


Figure S1. Absorptivity of **2** in various solvents

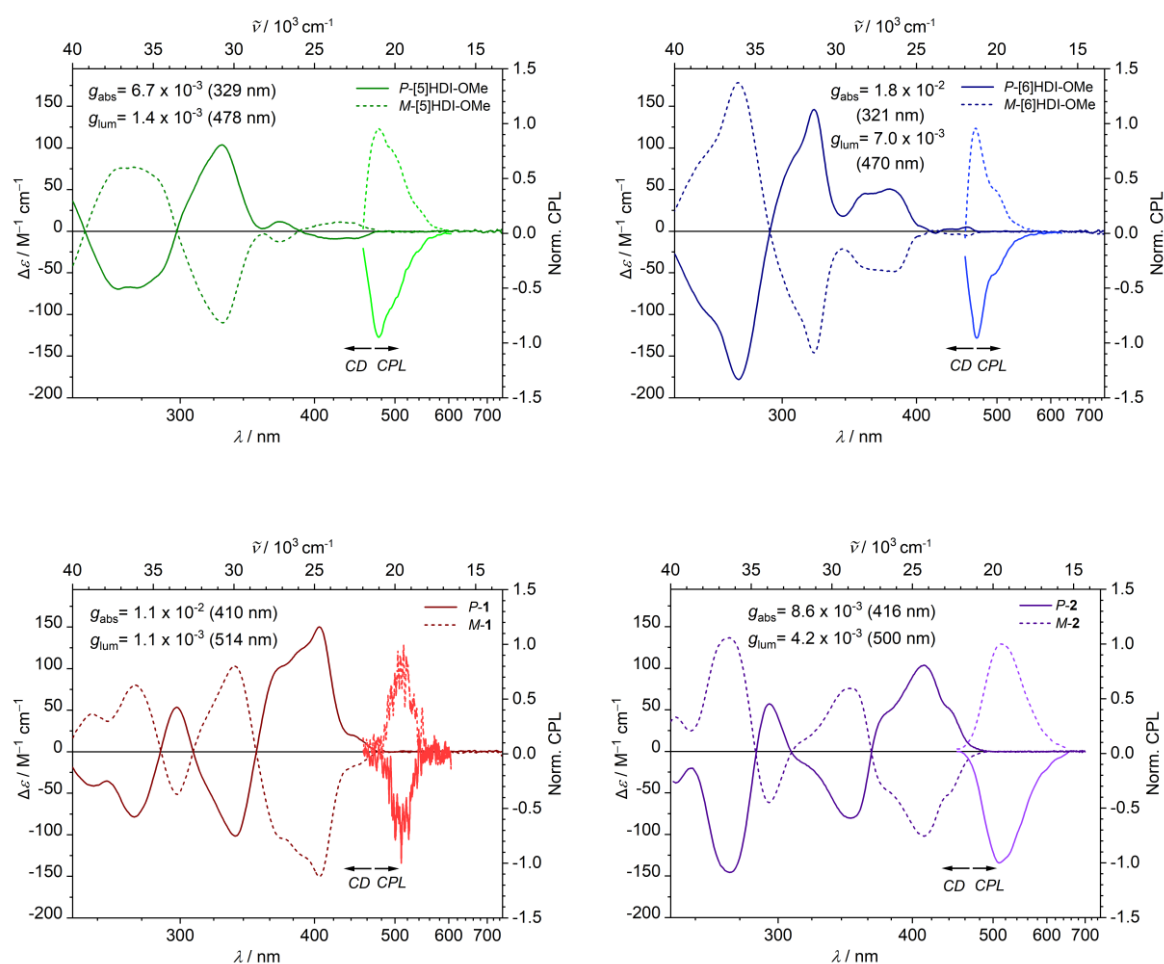


Figure S2. Electronic CD and CPL plots in chloroform for [5]HDI-OMe, [6]HDI-OMe², **1** and **2**. Excitation for the CPL measurements was at 400 nm. In our earlier paper² we did not report the CPL of [5]HDI-OMe, [6]HDI-OMe, and [7]HDI-OMe (**1**). To compare the CPL properties of these molecule with our new molecule **2** we report them here.

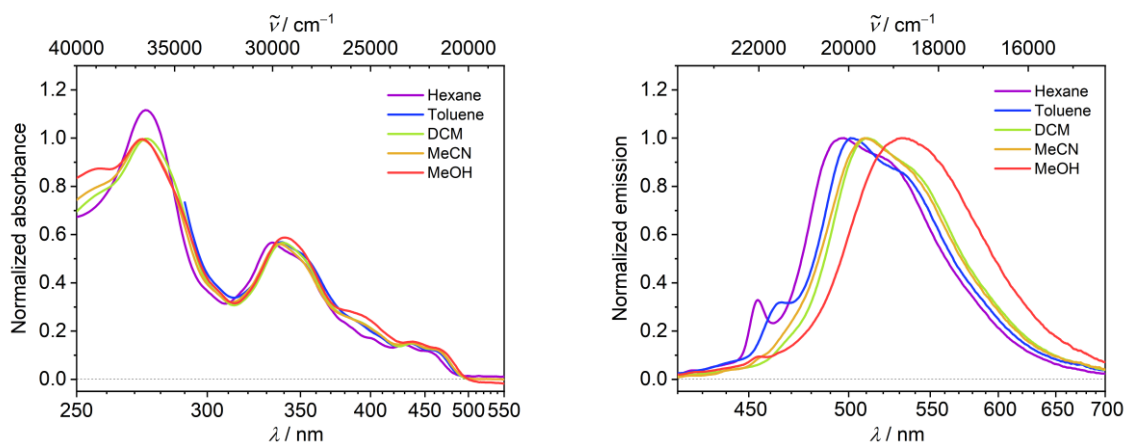


Figure S3. Absorption and emission spectra of **1** in solvents of varying polarity ($c \sim 10^{-6}$ M, excitation at 400 nm). In our earlier paper² we did not report absorption and emission plot for [7]HDI-OMe (**1**) in different solvents, to compare with **2**, we report them here.

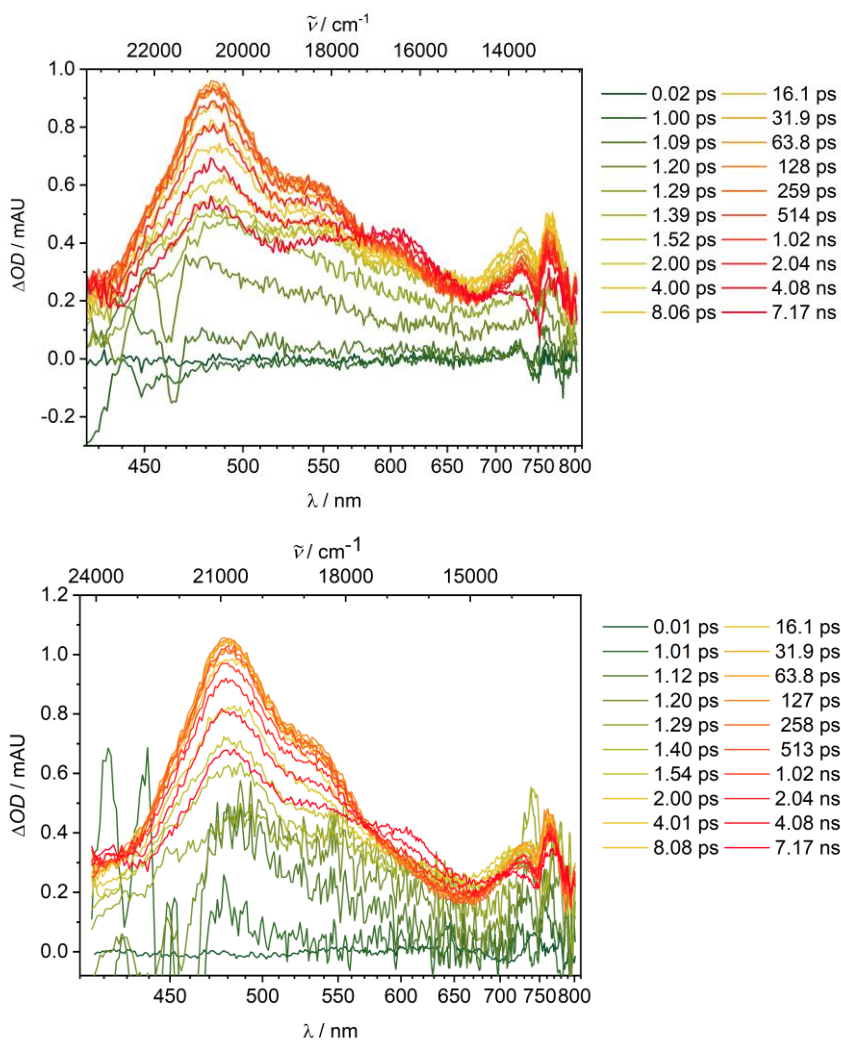


Figure S4. Selected transient absorption spectra in DCM (top) and MeCN (bottom).

S4. Cyclic Voltammetry and Spectroelectrochemistry

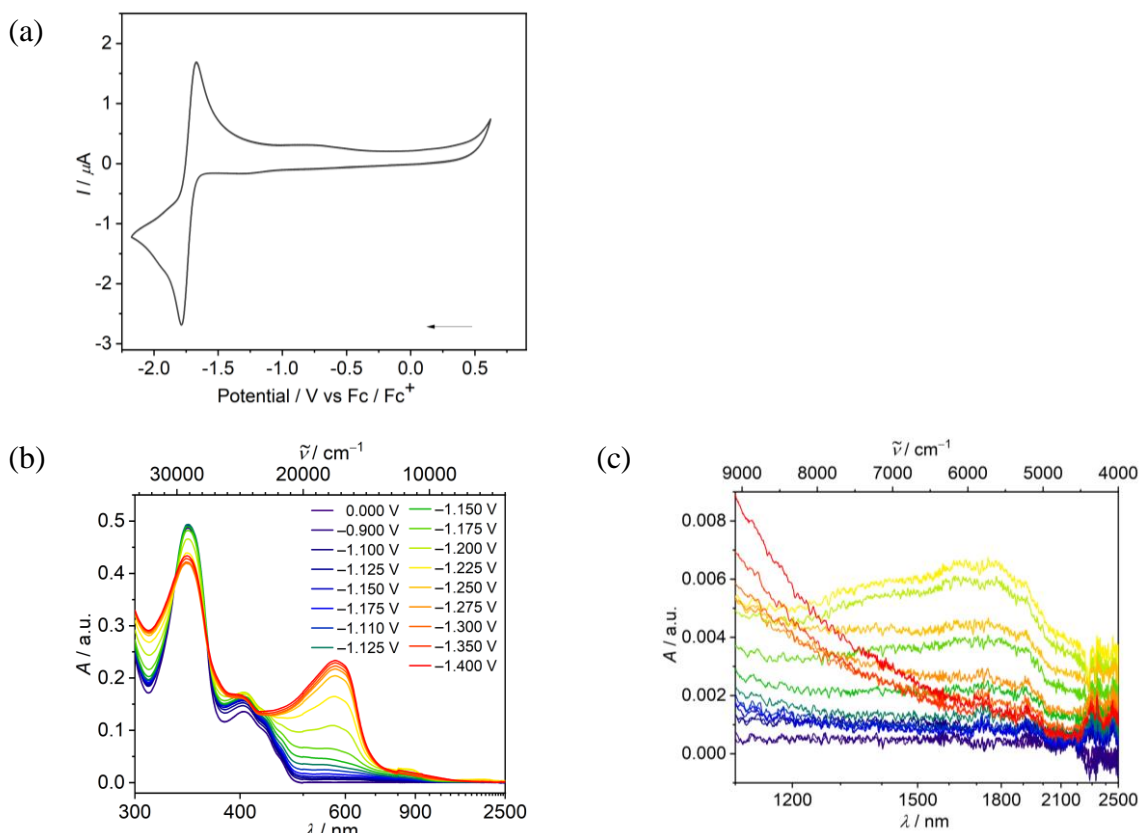


Figure S5. Electrochemical properties of **2**. (a) CV plot of **2** in THF (200 mV / s). (b) SEC spectra of **2** in THF. (c) Zoomed in section of graph b showing the weak band corresponding to the monoanion of **2**.

The reduction of **2** during SEC in THF (Fig. S5b) unveiled a swift spectral transition from the neutral compound to the reduced species at around -1.2 V, without exhibiting a two-step process. The resulting spectrum, featuring an absorption peak around 700 nm, is indicative of the dianionic species. Notably, a weak and broad absorption band around 1750 nm briefly appeared during the voltage change with the most significant spectrum alteration, signifying a transient presence of low concentrations of the radical monoanionic species (Fig. S5c). This indicates that the two reductions are distinct processes separated by a minor potential difference due to weak electronic coupling.

S5. Lippert-Mataga equation

The difference in dipole moment between the ground and excited states of **2** was estimated by Lippert-Mataga plot, in which the Stokes shift of the emission maximum is plotted against the Lippert-Mataga solvent function⁵: $\Delta f = f(D) - f(n^2) = \frac{\epsilon-1}{2\epsilon+1} - \frac{n^2-1}{2n^2+1}$, with the permittivity (dielectric constant), ϵ , and the refractive index, n , of the solvent. Using the linear fit equation from this plot (Fig. S3), it is possible to derive the difference in electric dipole moment between ground and excited states using the Lippert-Mataga equation:

$$\tilde{\nu}_A - \tilde{\nu}_E = \frac{2}{hc} (f(D) - f(n^2)) \frac{(\mu_e - \mu_g)^2}{a^3} + \text{constant}$$

where $\Delta\mu_{eg} = \mu_e - \mu_g$ is the difference between the molecular dipole moment in the excited and ground states, $\tilde{\nu}_A - \tilde{\nu}_E$ is the difference between the wavenumbers of the absorption and emission maxima and a is the spherical cavity radius of the solvent cage around the molecule.

Using $\frac{\epsilon-1}{2\epsilon+1} - \frac{n^2-1}{2n^2+1}$ as the x-axis, forming the derivative and solving for $\mu_e - \mu_g$ gives:

$$\mu_g - \mu_e = \sqrt{\frac{1}{2} (\Delta\tilde{\nu}_A - \Delta\tilde{\nu}_E) \cdot hc \cdot a^3}$$

With the values (in CGS units) of $\Delta\tilde{\nu}_A - \Delta\tilde{\nu}_E = 4927 \text{ cm}^{-1}$, $h = 6.6256 \times 10^{-27} \text{ erg s}$, $c = 2.9979 \times 10^{10} \text{ cm s}^{-1}$ and the value of a of 6.53 \AA (calculated using Gaussian), the calculation yields a notable change in dipole moment difference $\Delta\mu_{eg}$ of $11.7 \cdot 10^{-18} \text{ Fr cm} = 11.7 \text{ D}$.

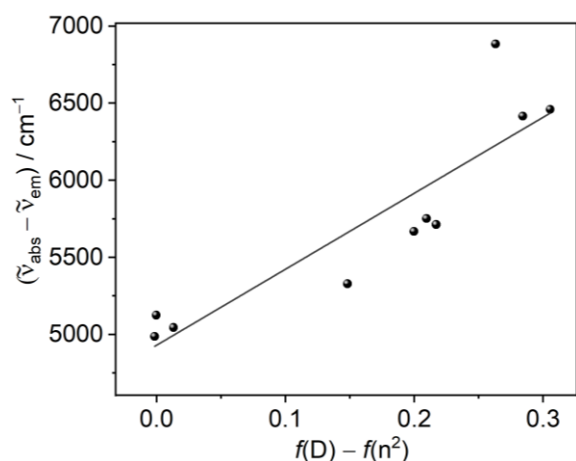


Figure S6. Lippert-Mataga plot of **2**.

S6. Chiral stationary phase HPLC

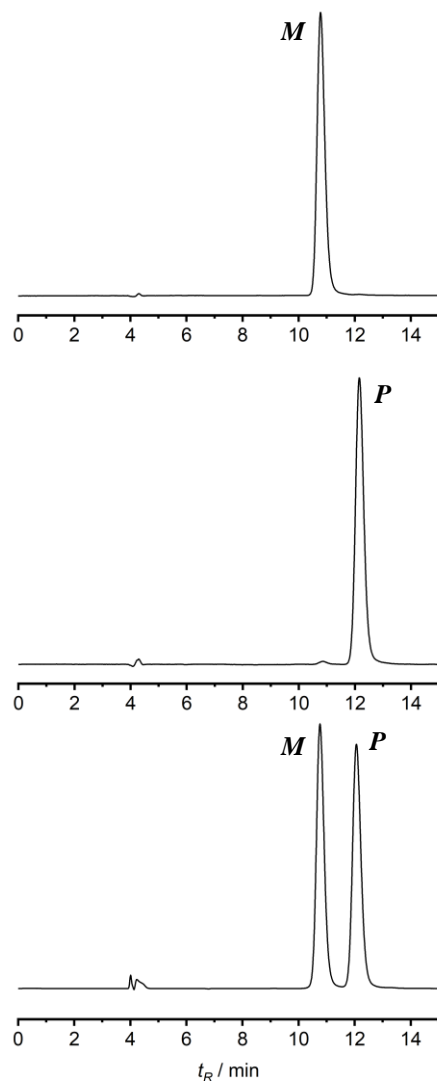


Figure S7. HPLC chromatogram of the diastereomeric mixture of **2** using a chiral stationary phase column. The chromatogram detector was set at 400 nm with a bandwidth of 4 nm.

Compound	column ^a	Eluent <i>n</i> -hex./CHCl ₃ / <i>i</i> PrOH	First fraction	Second fraction	α^b	R_s^c	<i>er</i>
2	Lux i-Amylose-3	73:25:2	<i>M</i>	<i>P</i>	1.12	4.20	>99%

^aPhenomenex Lux i-Amylose-3 5 μ m (250 x 4.6 mm). Sample injection: 10 μ L of a 0.5 mg/mL solution in CHCl₃. Separation conditions: Eluent, flow rate: 1 mL/min, 20 °C. ^bSelectivity parameter: $\alpha = t_{R2}/t_{R1}$, where t_{R1} , and t_{R2} are elution times for first fraction, and second fraction, respectively. ^cResolution parameter: $R_s = 2(t_{R2} - t_{R1})/(w_2 + w_1)$, where w_1 and w_2 are half-height peak widths for first and second fraction, respectively.

S7. Determination of barrier of enantiomerization

The value of the Gibbs activation energy ($\Delta G^\ddagger(T)$) for enantiomerization of **1** was calculated by following the decay of the enantiomeric excess (ee) of the enantioenriched samples dissolved in diphenyl ether at 513 K over time (t) by HPLC on a chiral stationary phase. To estimate the $\Delta G^\ddagger(T)$ value, the $\ln(ee_t/ee_0)$ values were plotted against t and the data set was linearly fitted (Figure S8). Following the equations $\ln(ee_t/ee_0) = -k_{\text{rac}}t$, where k_{rac} is the rate constant of racemization, and $k_{\text{rac}} = 2k_e$, where k_e is the rate constant of enantiomerization, the k_e values were obtained and used to calculate the corresponding $\Delta G^\ddagger(T)$ values by using the Eyring equation $\Delta G^\ddagger(T) = -RT \ln(k_e h / \kappa k_B T)$, where R is the gas constant ($R = 8.31446 \text{ J K}^{-1}$), h is the Planck constant ($h = 6.62607 \times 10^{-34} \text{ J} \cdot \text{s}$), k_B is the Boltzmann constant ($k_B = 1.38064852 \times 10^{-23} \text{ J K}^{-1}$), and κ is the transmission coefficient ($\kappa = 0.5$ or 1). The transmission coefficient $\kappa = 0.5$ was used because the enantiomerization process is defined as a reversible first order reaction.

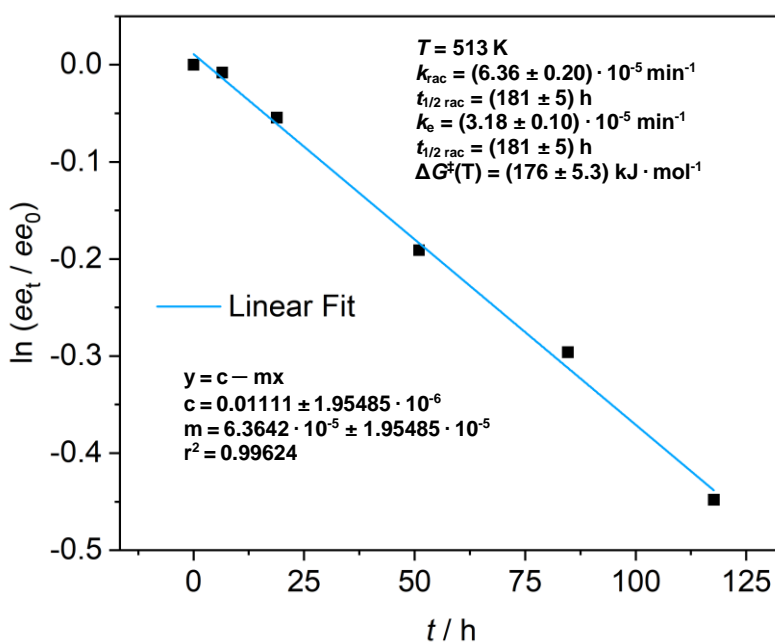


Fig. S8. Plot of $\ln(ee_t/ee_0)$ against t for **2** fitted linearly to obtain the k_d and $\Delta G^\ddagger(T)$ values.

S8. Quantum Chemical Calculations

DFT calculations were performed using Gaussian 16 suite.⁶ Geometries were optimized using ω B97XD functional and 6-31g(d,p) basis set. Frequency analysis was performed to verify the stationary state geometry, where no imaginary frequency was found. TD-DFT calculations were performed on ω B97XD/6-31g(d,p) optimized geometries at the B3LYP/6-31g(d,p) level. The effect of the solvent (DCM) was accounted using PCM. SpecDis⁷ and Avogadro/Chemcraft⁸ software were used to analyse the TD-DFT calculated spectra and to generate graphical images, respectively. To improve computing efficiency the *n*-butyl chains were replaced with methyl groups.

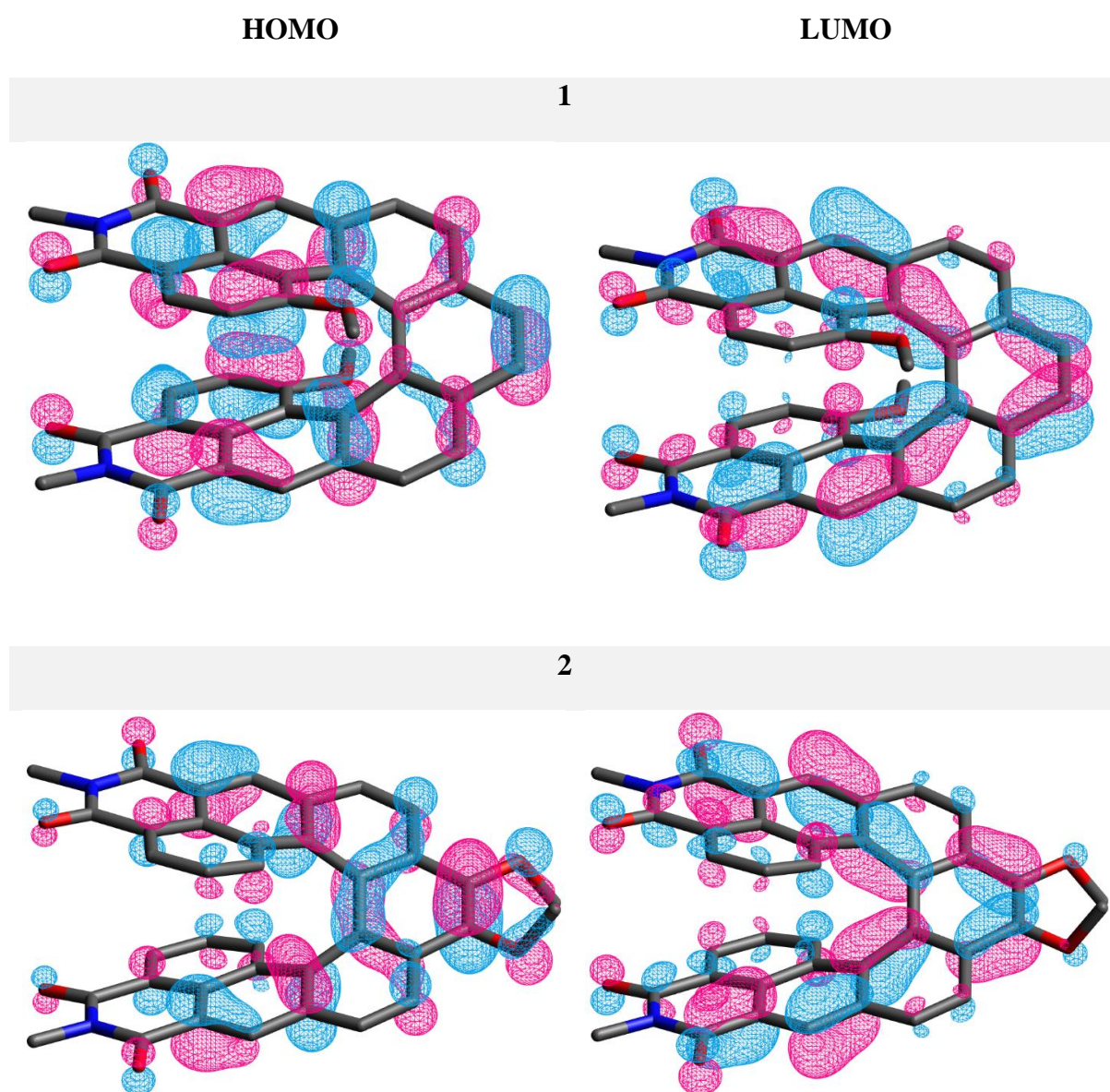


Figure S9. Frontier molecular orbitals of **1** and **2**.

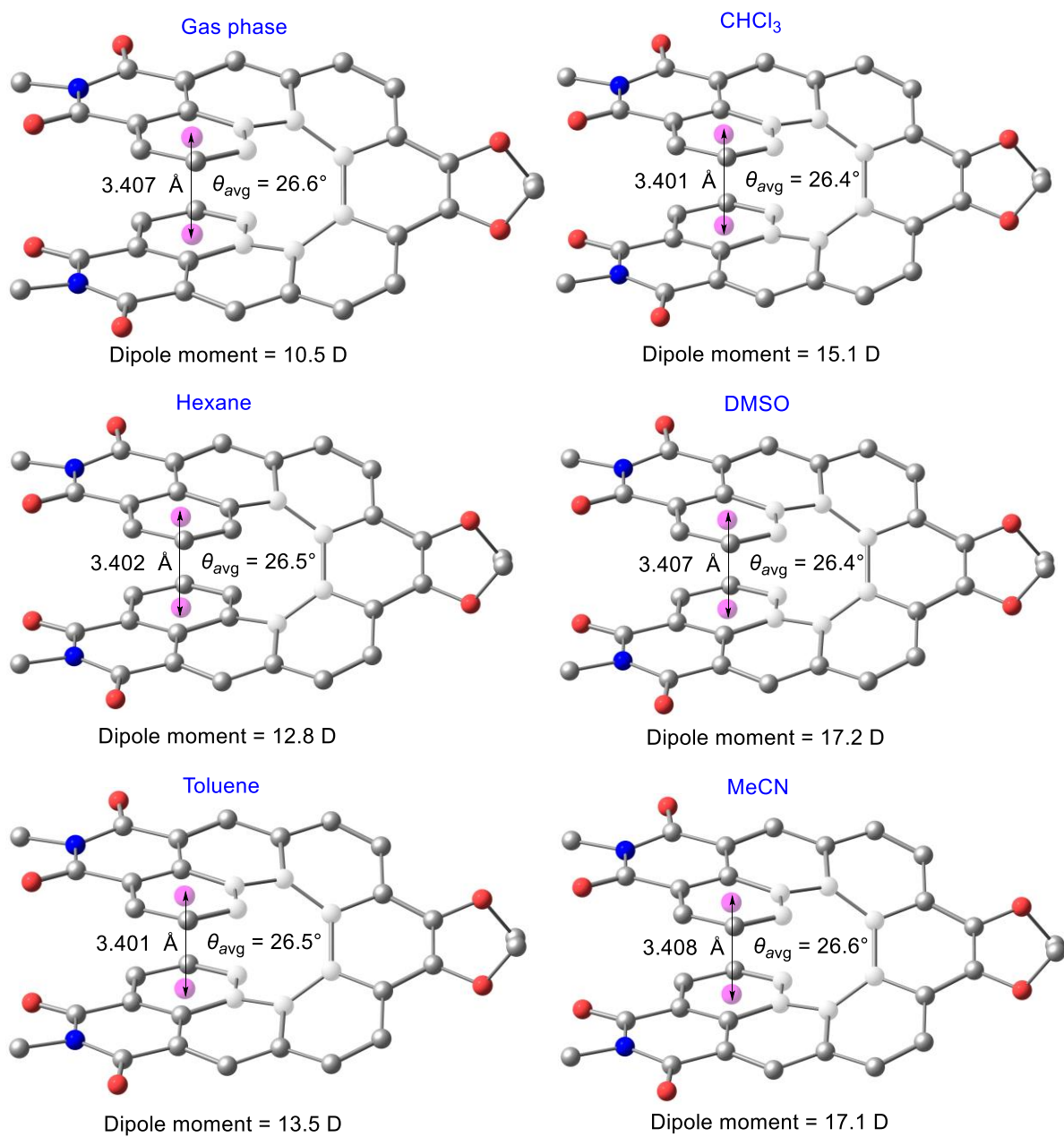


Figure S10. Optimized geometries of S_1 state for **2** in different solvents.

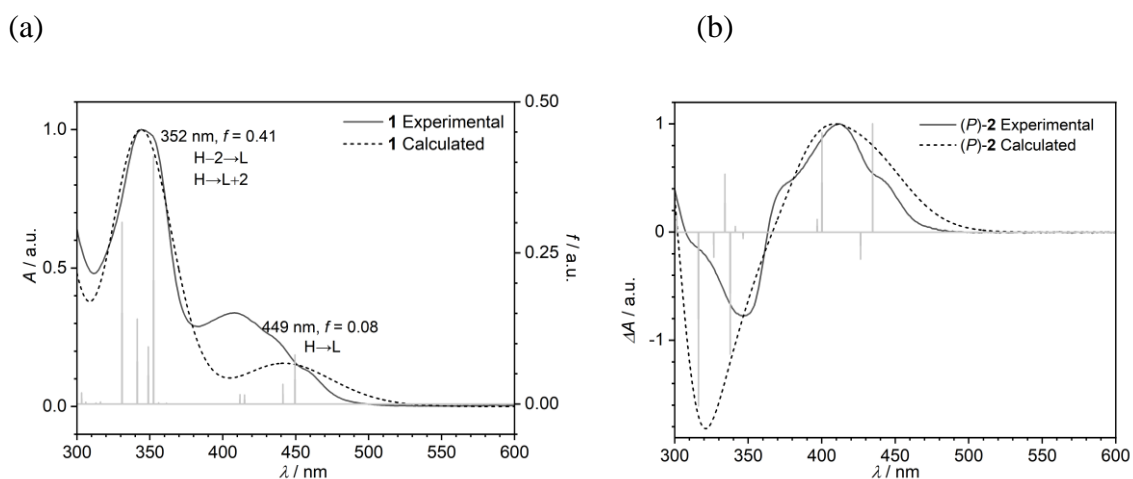


Figure S11. Comparison of experimental (solid) and TD-DFT calculated (dashed) (a) UV-vis absorption (shifted by 0.06 eV, 7 nm) (b) ECD spectra (shifted by 0.15 eV, 22 nm) of **2** along with assignments of key transitions. H = HOMO, L = LUMO, f = oscillator strength.

Table S2. Summary of TD-DFT calculated key transitions of **2**.

Excited singlet state	λ / nm	Energy/ eV	Major transitions	Contribution	oscillator strength (f)
1	449	2.76	HOMO→LUMO	0.70	0.08
2	441	2.81	HOMO-1→LUMO	0.52	0.03
			HOMO→LUMO+2	0.21	
7	352	3.52	HOMO-2→LUMO	0.45	0.41
			HOMO→LUMO+2	0.41	

Table S3. Calculated electric and magnetic transition dipole moments, and dissymmetry factor for $S_0 \rightarrow S_1$ and $S_1 \rightarrow S_0$ transitions for **1** and **2**.

Compd	$S_1 \leftarrow S_0$				$S_1 \rightarrow S_0$			
	$ \mu_e' / 10^{-20}$ esu cm	$ \mu_m' / 10^{-20}$ erg G ⁻¹	$ \cos\theta' $	$ g_{\text{abs}} / 10^{-3}$	$ \mu_e / 10^{-20}$ esu cm	$ \mu_m / 10^{-20}$ erg G ⁻¹	$ \cos\theta $	$ g_{\text{um}} / 10^{-3}$
1	256.86	2.23	0.06	2.0	253.38	2.45	0.03	1.3
2	281.13	2.45	0.19	6.7	277.05	2.31	0.10	3.2

Table S4. The inter valence-charge transfer (IV-CT) parameters calculated for radical anion using exact 35% HF-exchange contribution.

	$E_{\text{ab}} / \text{cm}^{-1}$	$\Delta\mu_{\text{ab}} / \text{D}$	$\mu_{\text{ab}} / \text{D}$	V_{12} / cm^{-1}	$\Delta G_{\text{ab}} / \text{cm}^{-1}$
1 (-1)	4155	3.77	1.64	1362	123.1
2 (-1)	3285	16.6	4.09	727	1708.7

$\Delta\mu_{\text{ab}}$: Dipole moment difference between ground state and IV-CT state, μ_{ab} : projection of transition moment on dipole moment difference vector $\Delta\mu_{\text{ab}}$. The IV-CT parameters for corresponding radical anions were obtained from (TD)-DFT calculations using a specially adjusted hybrid functional with an exact 35 % HF-exchange contribution. IVCT transition energy = reorganization energy (λ). Electronic coupling was calculated using the Mulliken–Hush formalism.⁹

S9. NMR spectroscopy

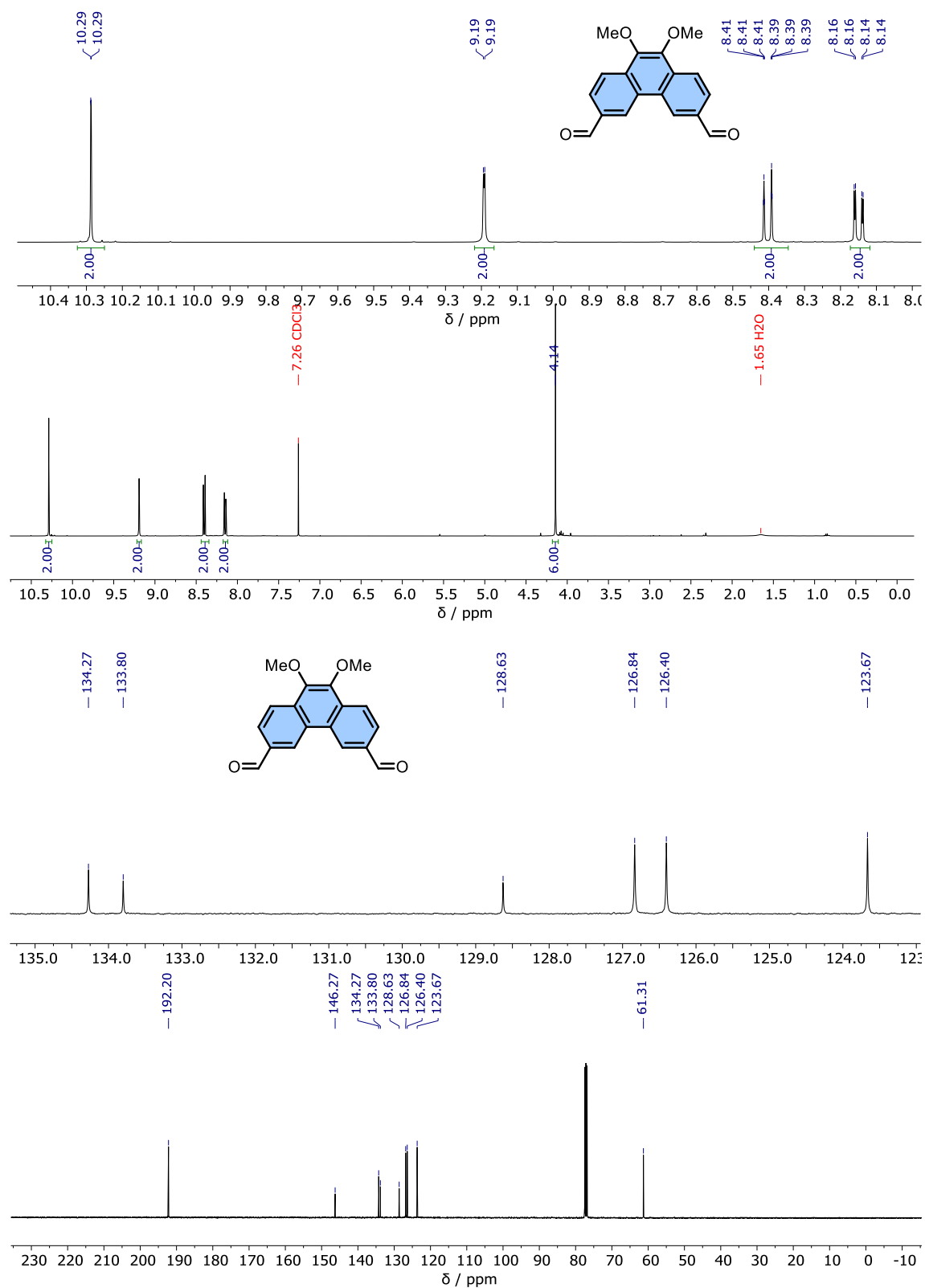


Figure S12. ¹H NMR spectrum of 9,10-dimethoxyphenanthrene-3,6-dicarbaldehyde (**4**) (400 MHz, CDCl₃, top) and ¹³C{¹H} NMR spectrum of 9,10-dimethoxyphenanthrene-3,6-dicarbaldehyde (101 MHz, CDCl₃, bottom).

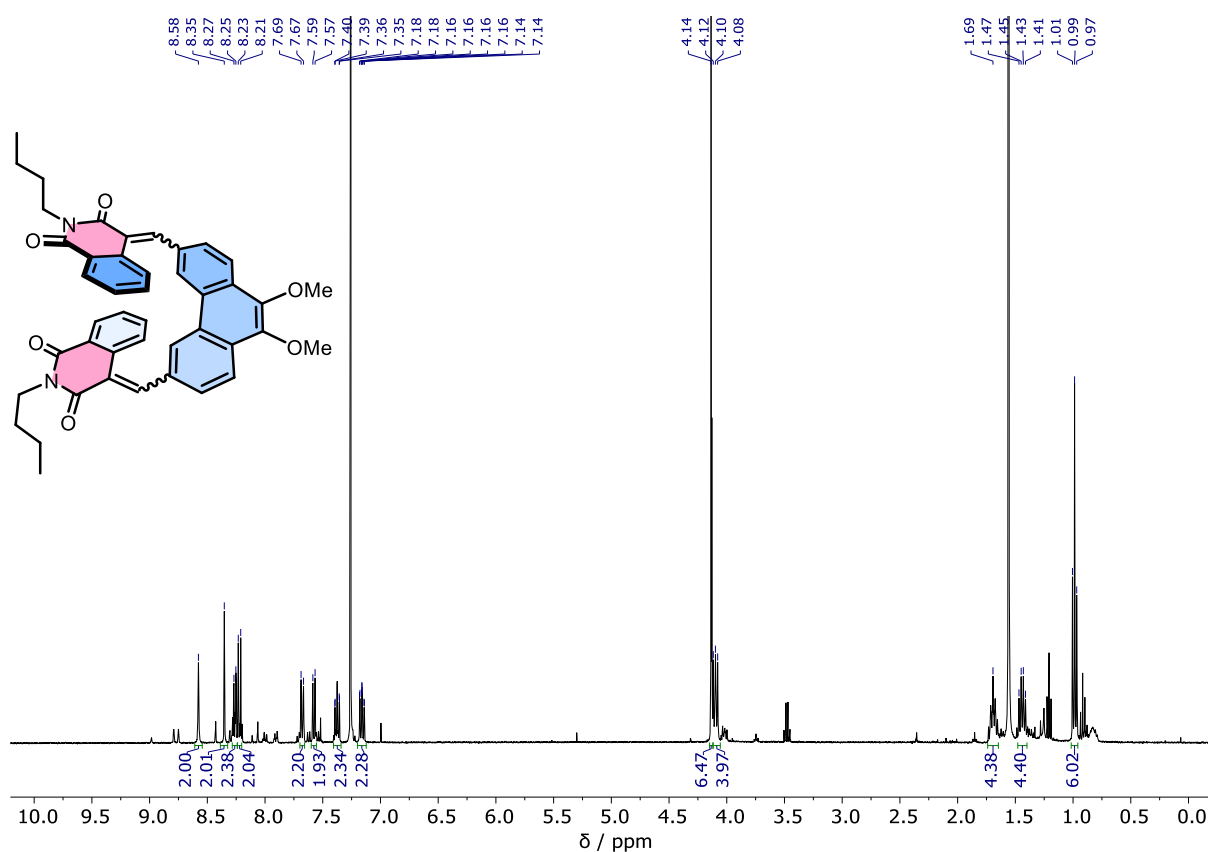


Figure S13. ^1H NMR spectrum of the major isomer of 4,4'-((9,10-dimethoxyphenanthrene-3,6-diyl)bis(methanelylidene))bis(2-butylisoquinoline-1,3(2H,4H)-dione) (**5**) (400MHz, CDCl_3). Since the minor isomers could not completely be removed, no further characterization was carried out. The purity of the sample was confirmed by HRMS (MALDI, *vide infra*).

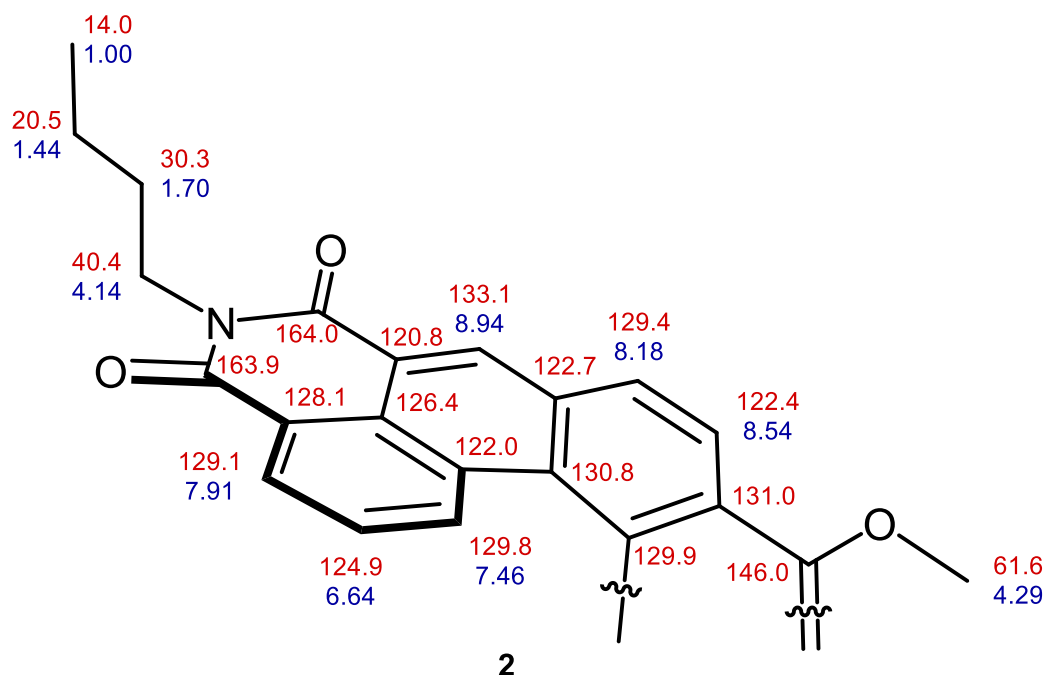


Figure S14. Assignment of ^1H (blue) and ^{13}C NMR (red) peaks to respective atoms in **2**.

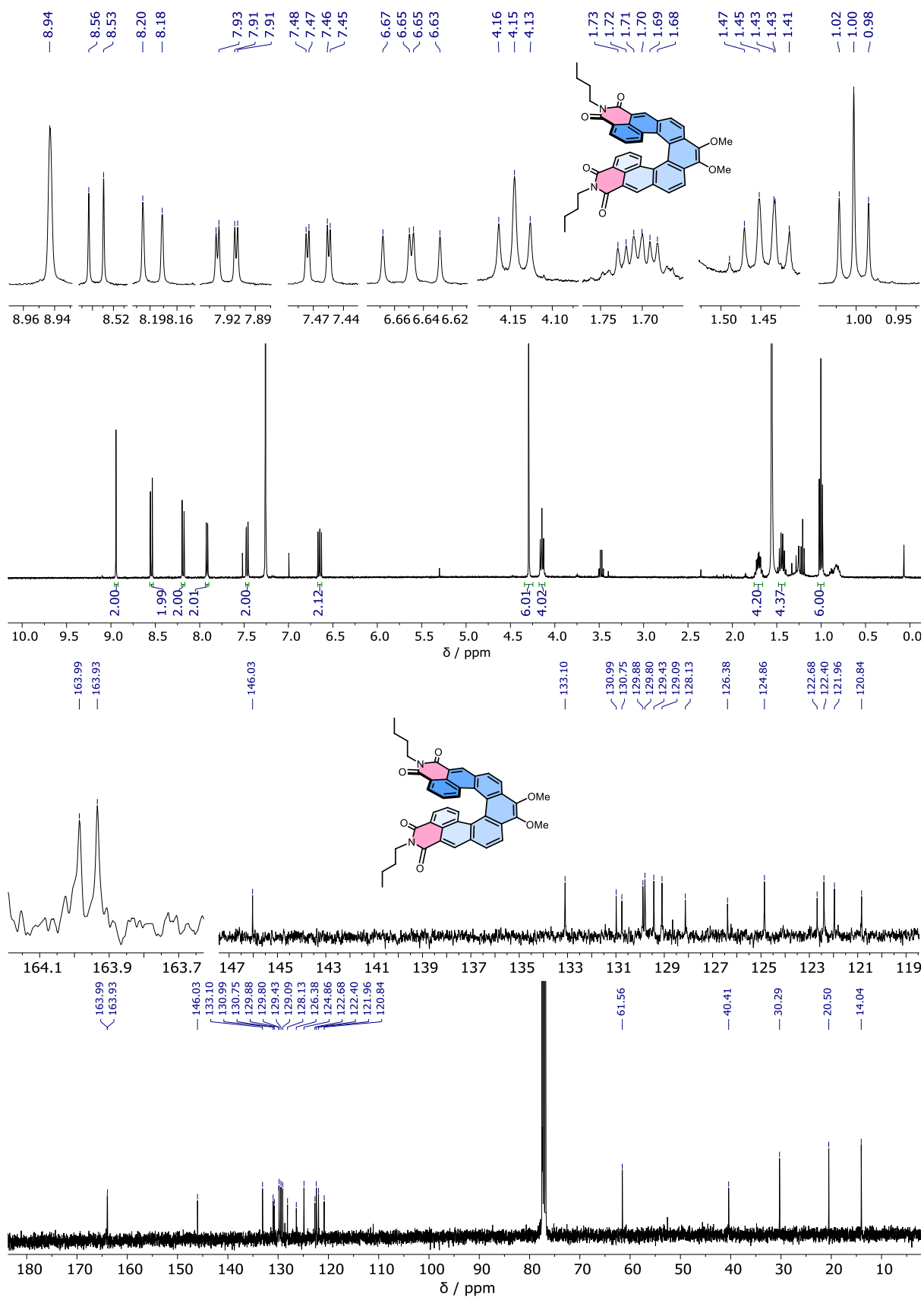


Figure S15. ¹H (top, 400MHz, CDCl₃) and ¹³C{¹H} NMR spectra (bottom, 101 MHz, CDCl₃) of **2**.

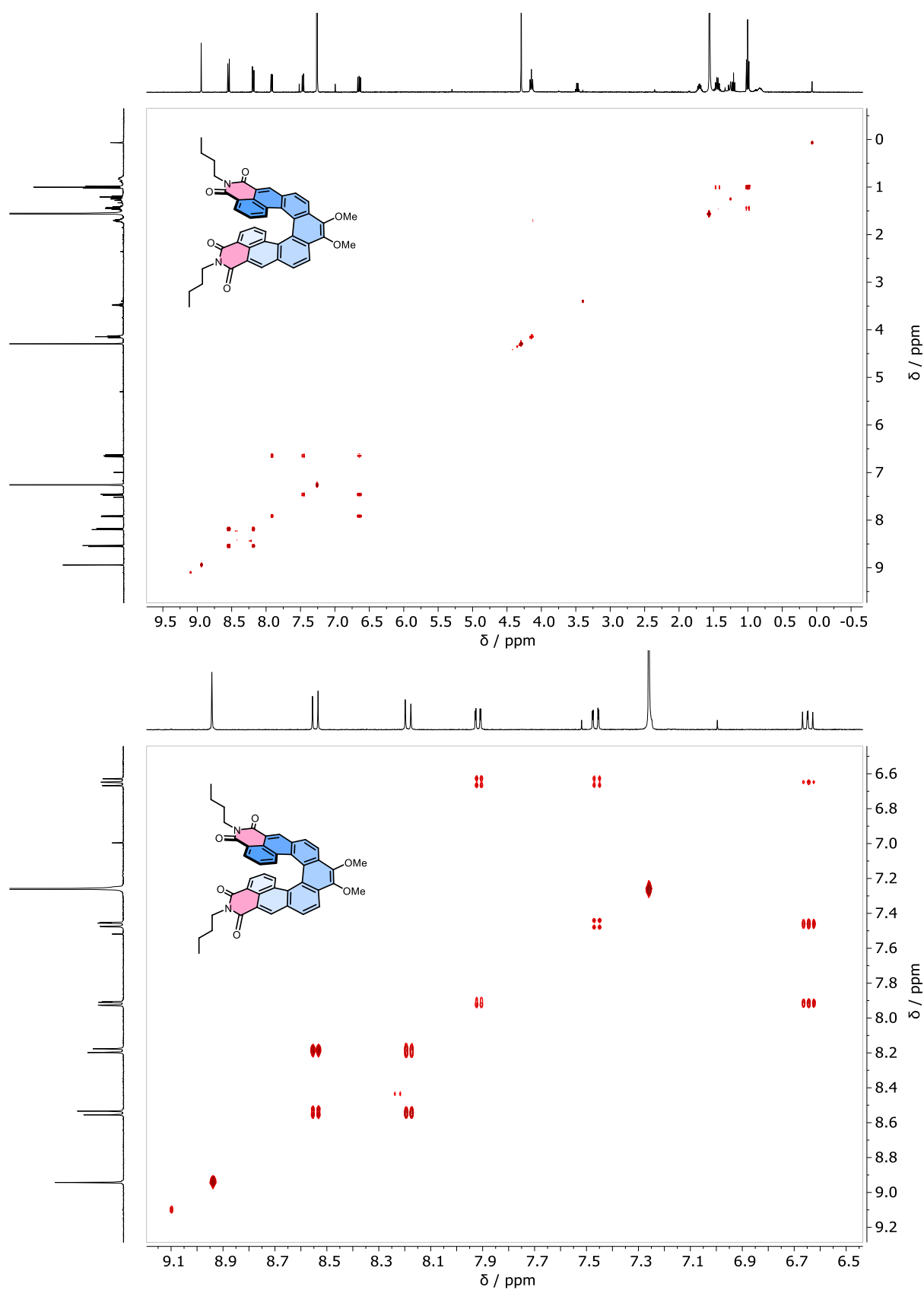


Figure S16. ^1H - ^1H COSY NMR spectrum of **2** (top), magnified aromatic section (bottom).

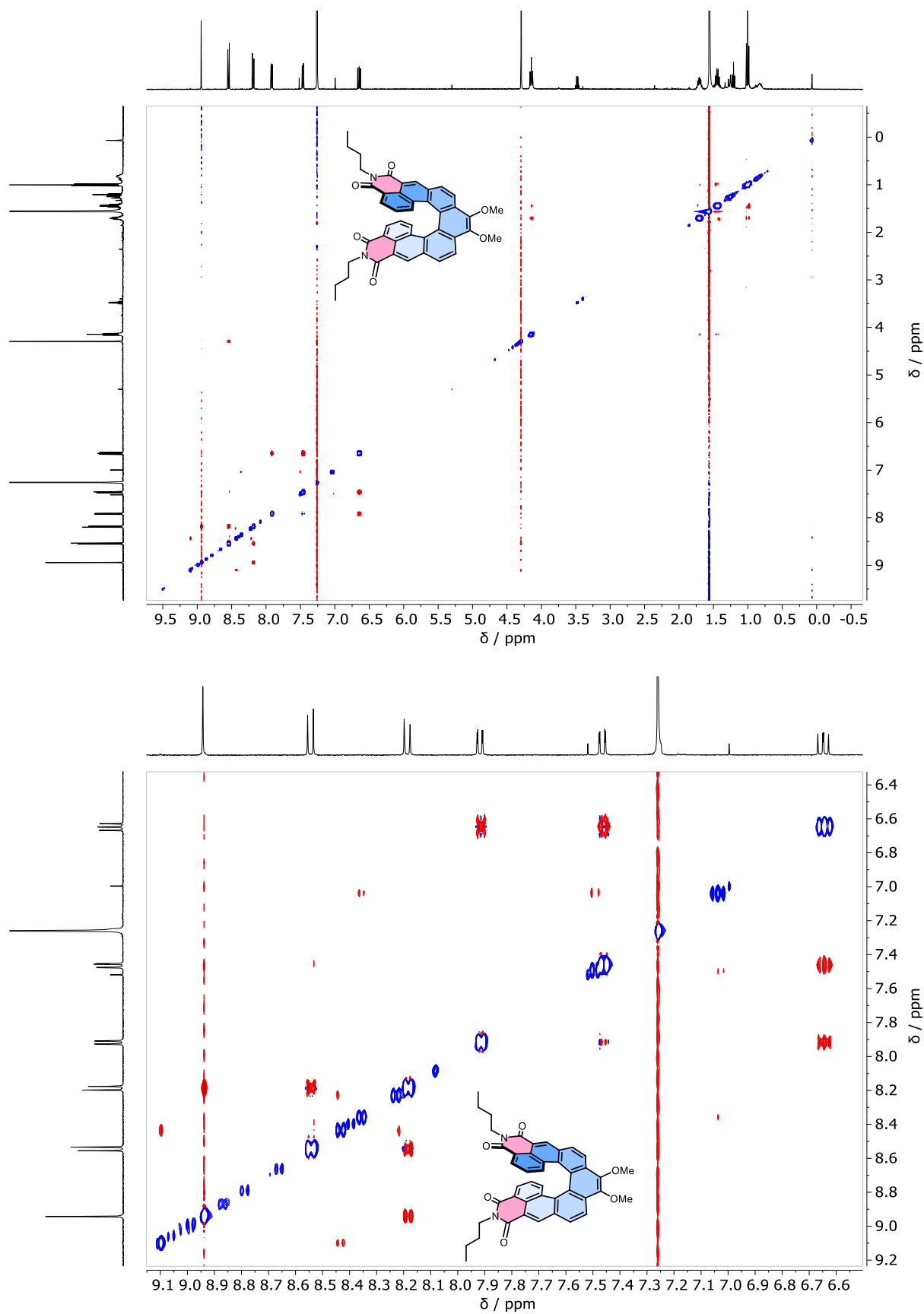


Figure S17. ^1H - ^1H NOESY NMR spectrum of **2** (top), magnified aromatic section (bottom).

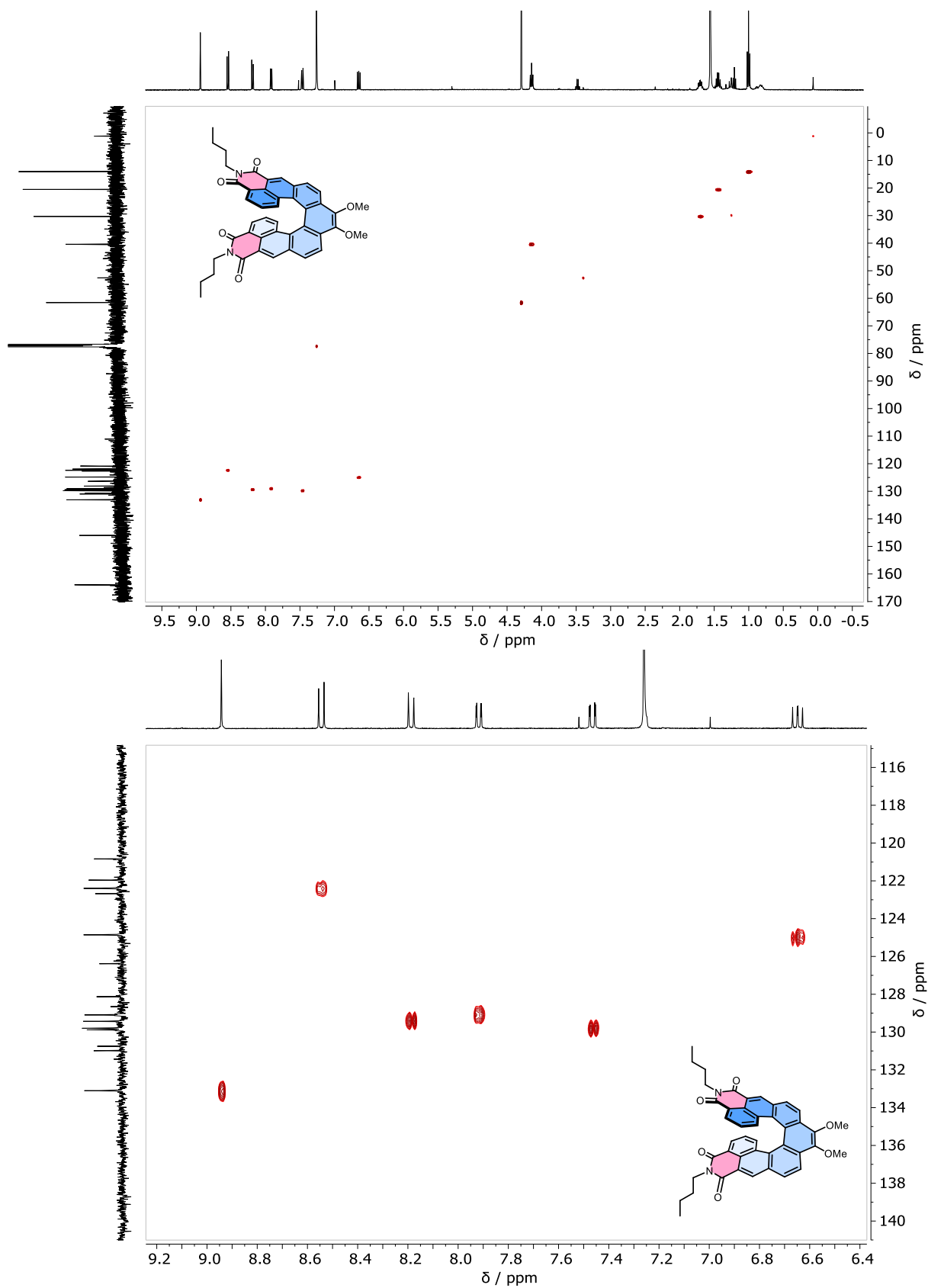


Figure S18. ^1H - ^{13}C HSQC NMR spectrum of **2** (top), magnified aromatic section (bottom).

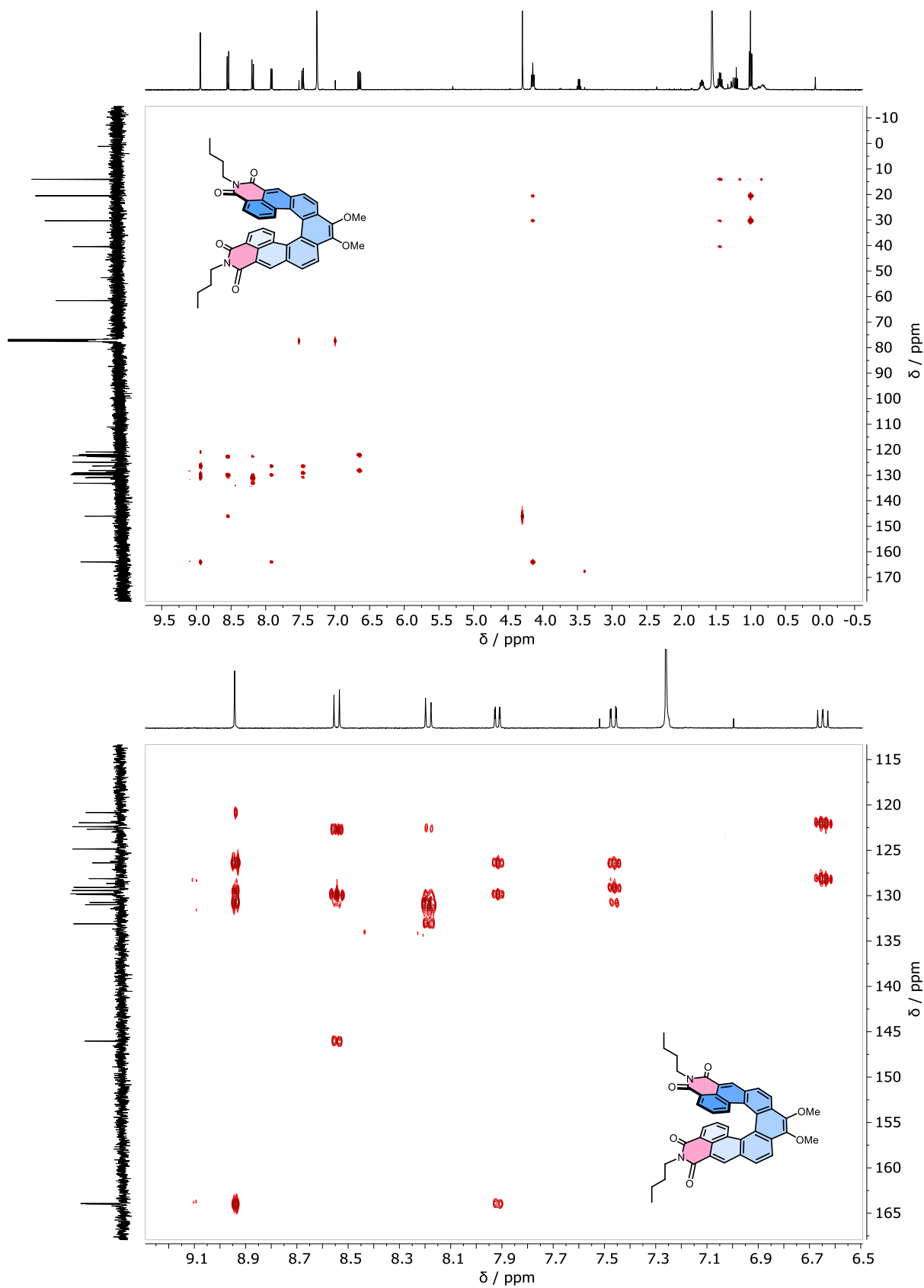


Figure S19. ^1H - ^{13}C HMBC NMR spectrum of **2**, magnified aromatic section (bottom).

S10. High-resolution mass spectrometry (HRMS)

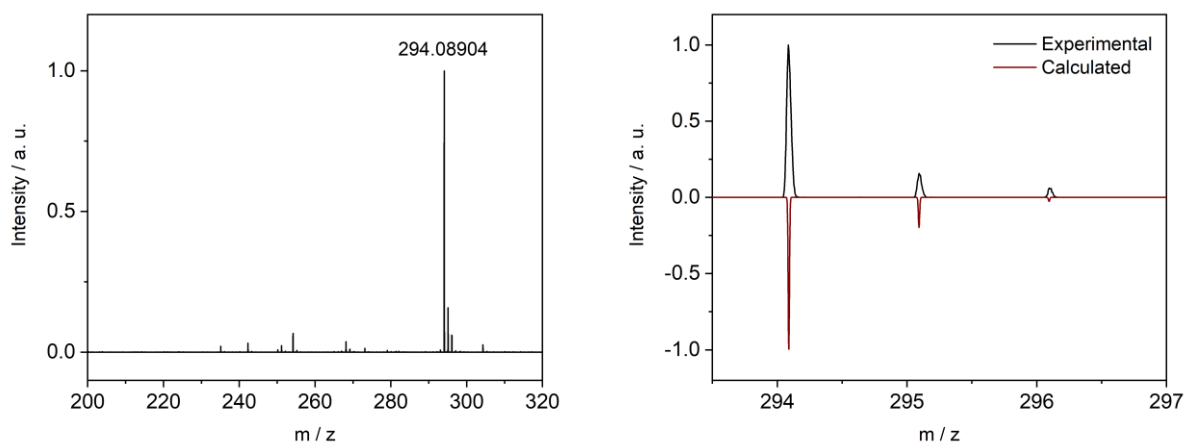


Figure S20. MALDI-TOF HRMS of 4.

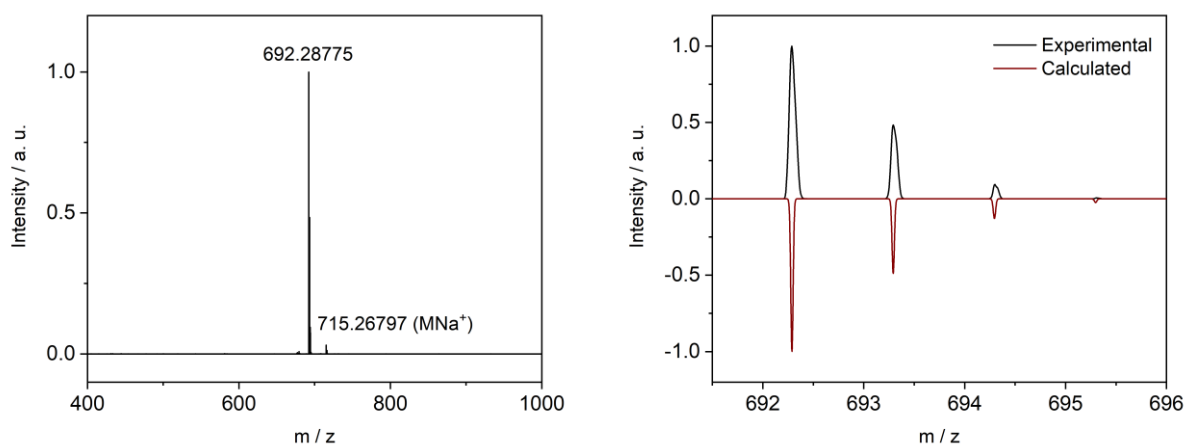


Figure S21. MALDI-TOF HRMS of 5.

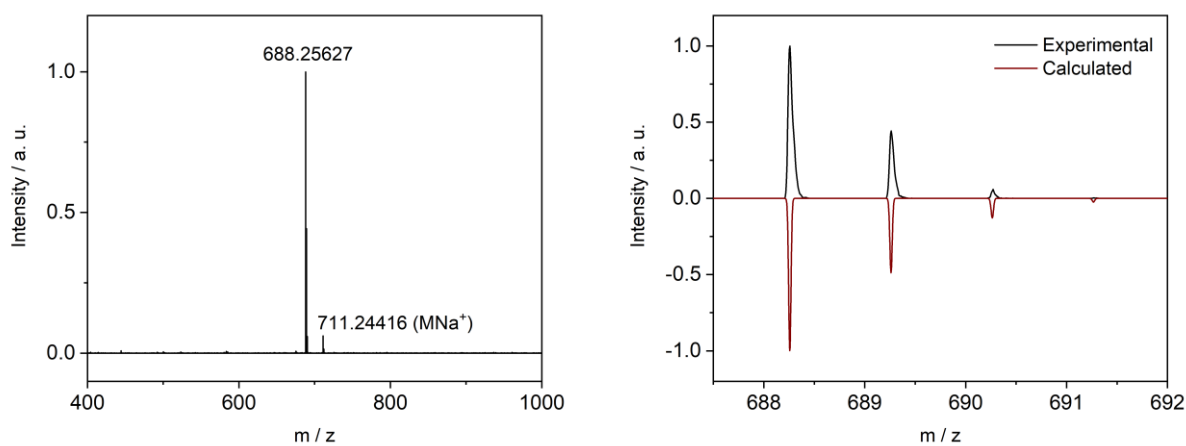


Figure S22. MALDI-TOF HRMS of 2.

S11. Cartesian Coordinates

1

C	0.177822000	-0.699137000	2.844692000	C	-0.552468000	2.779974000	-0.792004000	H	2.988174000	1.906333000	-0.620738000
C	-0.177822000	0.699137000	2.844692000	C	-0.310444000	3.461675000	0.362582000	H	0.062173000	4.575973000	2.796369000
C	0.074877000	-1.409245000	4.053985000	C	-1.500083000	0.828810000	-1.929764000	H	0.070244000	3.374198000	4.961532000
C	-0.074877000	1.409245000	4.053985000	C	-2.135950000	-0.392680000	-1.875954000	H	-0.009885000	4.503631000	0.305884000
C	0.011999000	0.679850000	5.281246000	C	-2.424600000	-0.982928000	-0.643709000	H	-2.437111000	-0.866729000	-2.803582000
C	-0.011999000	-0.679850000	5.281246000	C	-2.002067000	-0.386010000	0.535232000	H	-2.988174000	-1.906333000	-0.620738000
C	0.044466000	-2.834466000	4.026237000	C	-1.235418000	1.450741000	-3.241190000	H	1.225183000	-3.495094000	-5.083930000
C	0.596500000	-1.412795000	1.666953000	C	-0.298937000	3.440077000	-2.096841000	H	-0.270666000	-4.180773000	-4.390550000
C	0.351557000	-2.799127000	1.625805000	C	1.235418000	-1.450741000	-3.241190000	H	-0.268794000	-2.544588000	-5.129352000
C	0.074415000	-3.499548000	2.837353000	C	0.298937000	-3.440077000	-2.096841000	H	0.268794000	2.544588000	-5.129352000
C	0.310444000	-3.461675000	0.362582000	N	0.604537000	-2.700496000	-3.237888000	H	-1.225183000	3.495094000	-5.083930000
C	0.552468000	-2.779974000	-0.792004000	C	0.301227000	-3.269840000	-4.547411000	H	0.270666000	4.180773000	-4.390550000
C	1.082652000	-1.455128000	-0.737935000	N	-0.604537000	2.700496000	-3.237888000	C	3.049252000	2.060365000	1.859271000
C	1.212885000	-0.804346000	0.504512000	C	-0.301227000	3.269840000	-4.547411000	H	3.127574000	2.262856000	2.926694000
C	1.500083000	-0.828810000	-1.929764000	O	0.177822000	4.559591000	-2.171500000	H	4.051284000	1.969521000	1.424259000
C	2.135950000	0.392680000	-1.875954000	O	-1.527014000	0.919006000	-4.296524000	H	2.508691000	2.881811000	1.376074000
C	2.424600000	0.982928000	-0.643709000	O	-0.177822000	-4.559591000	-2.171500000	C	-3.049252000	-2.060365000	1.859271000
C	2.002067000	0.386010000	0.535232000	O	1.527014000	-0.919006000	-4.296524000	H	-3.127574000	-2.262856000	2.926694000
C	-0.596500000	1.412795000	1.666953000	H	0.040936000	1.233795000	6.214849000	H	-4.051284000	-1.969521000	1.424259000
C	-0.351557000	2.799127000	1.625805000	H	-0.040936000	-1.233795000	6.214849000	H	-2.508691000	-2.881811000	1.376074000
C	-0.074415000	3.499548000	2.837353000	H	-0.070244000	-3.374198000	4.961532000	O	2.332319000	0.847818000	1.754191000
C	-0.044466000	2.834466000	4.026237000	H	-0.062173000	-4.575973000	2.796369000	O	-2.332319000	-0.847818000	1.754191000
C	-1.212885000	0.804346000	0.504512000	H	0.009885000	-4.503631000	0.305884000				
C	-1.082652000	1.455128000	-0.737935000	H	2.437111000	0.866729000	-2.803582000				

1 Excited State S₁

C	0.185347000	-0.702249000	2.837888000	C	-1.422882000	0.694336000	-1.929893000	H	-2.388099000	-0.995968000	-2.792416000
C	-0.185925000	0.702484000	2.837784000	C	-2.104599000	-0.506884000	-1.867264000	H	-2.975089000	-1.996757000	-0.607730000
C	0.047687000	-1.423752000	4.065080000	C	-2.418580000	-1.069309000	-0.636461000	H	0.795180000	-3.227460000	-5.157197000
C	-0.048486000	1.424106000	4.064923000	C	-2.020298000	-0.445417000	0.554161000	H	-0.700018000	-3.819873000	-4.381012000
C	0.023836000	0.699457000	5.255109000	C	-1.093458000	1.271934000	-3.244359000	H	-0.612394000	-2.153960000	-5.051473000
C	-0.024896000	-0.698980000	5.255172000	C	-0.075978000	3.220065000	-2.103513000	H	0.613322000	2.153557000	-5.051650000
C	0.039824000	-2.861178000	4.020683000	C	1.094045000	-1.272229000	-3.243999000	H	-0.794329000	3.226925000	-5.157655000
C	0.654023000	-1.372655000	1.696403000	C	0.076467000	-3.220307000	-2.103154000	H	0.700722000	3.819531000	-4.381319000
C	0.401750000	-2.785819000	1.619755000	N	0.373372000	-2.466435000	-3.241448000	C	3.039387000	2.151988000	1.866721000
C	0.134737000	-3.509169000	2.834111000	C	-0.066339000	-2.952023000	-4.545626000	H	3.121276000	2.355668000	2.933619000
C	0.265137000	-3.375957000	0.363334000	N	-0.372724000	2.466110000	-3.241785000	H	4.040649000	2.075650000	1.427645000
C	0.451726000	-2.632197000	-0.803494000	C	0.067133000	2.951617000	-4.545945000	H	2.483162000	2.964559000	1.386084000
C	1.039809000	-1.350101000	-0.737370000	O	0.493585000	4.298632000	-2.185532000	C	-3.039592000	-2.151892000	1.866332000
C	1.239004000	-0.731806000	0.521687000	O	-1.397678000	0.735871000	-4.296928000	H	-3.121319000	-2.355671000	2.933224000
C	1.423218000	-0.694498000	-1.929530000	O	-0.493083000	-4.298879000	-2.185180000	H	-4.040921000	-2.075651000	1.427393000
C	2.104841000	0.506776000	-1.866888000	O	1.398403000	-0.736223000	-4.296561000	H	-2.483331000	-2.964357000	1.385563000
C	2.418590000	1.069321000	-0.636082000	H	0.064537000	1.235661000	6.198617000	O	2.338293000	0.928276000	1.768042000
C	2.020137000	0.445504000	0.554528000	H	-0.065775000	-1.235091000	6.198726000	O	-2.338701000	-0.928056000	1.767664000
C	-0.654320000	1.372797000	1.696122000	H	-0.098749000	-3.410746000	4.947032000				
C	-0.401945000	2.785937000	1.619381000	H	0.025488000	-4.587952000	2.775877000				
C	-0.135116000	3.509395000	2.833711000	H	-0.056979000	-4.408447000	0.270723000				
C	-0.040516000	2.861525000	4.020374000	H	2.388482000	0.995790000	-2.792033000				
C	-1.239100000	0.731859000	0.521350000	H	2.975016000	1.996818000	-0.607334000				
C	-1.039661000	1.350029000	-0.737726000	H	-0.025801000	4.588167000	2.775392000				
C	-0.451485000	2.632087000	-0.803861000	H	0.097892000	3.411181000	4.946695000				
C	-0.265060000	3.375939000	0.362926000	H	0.057145000	4.408399000	0.270279000				

2

C	2.302195000	-0.718808000	-0.075800000	C	-1.307341000	2.907617000	0.295178000	H	-1.088833000	1.574872000	-3.094460000
C	2.302195000	0.718779000	0.075907000	C	-0.149965000	3.528184000	-0.069059000	H	2.286857000	4.540250000	-0.655662000
C	3.515172000	-1.407615000	0.123641000	C	-2.436007000	1.062299000	1.457048000	H	4.441519000	3.316812000	-0.538398000
C	3.515178000	1.407576000	-0.123523000	C	-2.383588000	-0.102678000	2.194399000	H	-0.196701000	4.535866000	-0.470502000
C	4.745419000	0.676107000	-0.119514000	C	-1.141876000	-0.694104000	2.464135000	H	-3.308107000	-0.521885000	2.575550000
C	4.745425000	-0.676156000	0.119626000	C	0.012162000	-0.170067000	1.922102000	H	-1.088915000	-1.574864000	3.094499000
C	3.500165000	-2.816157000	0.348027000	C	-3.749355000	1.700886000	1.202833000	H	-5.539066000	-3.766849000	-1.180832000
C	1.131395000	-1.496545000	-0.391757000	C	-2.606202000	3.586697000	0.065286000	H	-4.902955000	-4.390539000	0.368313000
C	1.101887000	-2.844991000	0.005777000	C	-3.749337000	-1.700864000	-1.202861000	H	-5.685957000	-2.779233000	0.281609000
C	2.316838000	-3.488863000	0.386789000	C	-2.606220000	-3.586701000	-0.065322000	H	-5.685934000	2.779250000	-0.281705000
C	-0.149985000	-3.528202000	0.069086000	N	-3.747366000	-2.907059000	-0.496322000	H	-5.539075000	3.766870000	1.180737000
C	-1.307349000	-2.907623000	-0.295169000	C	-5.055792000	-3.501850000	-0.238449000	H	-4.902922000	4.390552000	-0.368394000
C	-1.257522000	-1.634684000	-0.938508000	N	-3.747362000	2.907071000	0.496277000	H	0.964629000	-0.637594000	2.140655000
C	-0.025254000	-0.966834000	-1.085378000	C	-5.055779000	3.501866000	0.238368000	H	0.964683000	0.637591000	-2.140562000
C	-2.435979000	-1.062289000	-1.457049000	O	-2.682527000	4.669666000	-0.486871000	C	6.689700000	1.026629000	-1.396771000
C	-2.383535000	0.102690000	-2.194397000	O	-4.799650000	1.213576000	1.575573000	C	6.690126000	-1.026455000	1.396397000
C	-1.141813000	0.694110000	-2.464100000	O	-2.682562000	-4.669683000	0.486808000	H	7.537064000	1.712593000	-1.408686000
C	0.012209000	0.170066000	-1.922039000	O	-4.799621000	-1.213539000	-1.575612000	H	6.111200000	1.143918000	-2.319620000
C	1.131394000	1.496525000	0.391835000	O	5.901130000	1.389326000	-0.265366000	H	7.045525000	-0.004643000	-1.318932000
C	1.101902000	2.844967000	-0.005712000	O	5.901100000	-1.389421000	0.265395000	H	7.537195000	-1.712780000	1.408442000
C	2.316865000	3.488831000	-0.386701000	H	4.441488000	-3.316858000	0.538534000	H	6.111820000	-1.143013000	2.319459000
C	3.500187000	2.816118000	-0.347915000	H	2.286819000	-4.540281000	0.655749000	H	7.046351000	0.004627000	1.317932000
C	-0.025274000	0.966828000	1.085434000	H	-0.196737000	-4.535888000	0.470516000				
C	-1.257536000	1.634684000	0.938530000	H	-3.308042000	0.521904000	-2.575569000				

2 Excited State S₁

C	-0.714025000	-0.157301000	2.337725000	C	2.652314000	0.436122000	-1.305288000	H	1.975434000	-2.963205000	-0.970400000
C	0.714047000	0.157341000	2.337738000	C	3.391828000	0.200246000	-0.145697000	H	4.587402000	-0.188116000	2.263663000
C	-1.433874000	0.045182000	3.558448000	C	0.694514000	1.441748000	-2.388617000	H	3.403349000	-0.324293000	4.434273000
C	1.433886000	-0.045167000	3.558462000	C	-0.506698000	2.122812000	-2.300043000	H	4.414220000	-0.148980000	-0.249990000
C	0.706792000	-0.090125000	4.749074000	C	-1.048146000	2.406263000	-1.045110000	H	-1.004859000	2.423272000	-3.215019000
C	-0.706791000	0.090124000	4.749068000	C	-0.412189000	1.968693000	0.111442000	H	-1.975378000	2.963299000	-0.970351000
C	-2.867975000	0.132766000	3.512005000	C	1.255291000	1.125902000	-3.718938000	H	-3.166846000	-0.879257000	-5.667572000
C	-1.406191000	-0.606665000	1.206069000	C	3.230386000	0.100366000	-2.620250000	H	-3.812557000	0.609364000	-4.920726000
C	-2.808580000	-0.309828000	1.118827000	C	-1.255301000	-1.125905000	-3.718971000	H	-2.132566000	0.557531000	-5.557349000
C	-3.515092000	0.028823000	2.324140000	C	-3.230387000	-0.100359000	-2.620274000	H	2.132485000	-0.557623000	-5.557278000
C	-3.391812000	-0.200234000	-0.145719000	N	-2.455649000	-0.417202000	-3.742403000	H	3.166773000	0.879155000	-5.667567000
C	-2.652303000	-0.436106000	-1.305316000	C	-2.926092000	-0.003883000	-5.061249000	H	3.812490000	-0.609450000	-4.920694000
C	-1.373412000	-1.030275000	-1.220708000	N	2.455619000	0.417164000	-3.742370000	H	-0.852652000	2.185745000	1.078365000
C	-0.764247000	-1.215286000	0.043972000	C	2.926027000	0.003799000	-5.061214000	H	0.852712000	-2.185655000	1.078321000
C	-0.694498000	-1.441713000	-2.388654000	O	4.313445000	-0.452821000	-2.733030000	C	1.075199000	-1.367787000	6.694951000
C	0.506732000	-2.122748000	-2.300085000	O	0.698261000	1.435129000	-4.758318000	C	-1.075224000	1.367749000	6.694964000
C	1.048196000	-2.406178000	-1.045155000	O	-4.313494000	0.452732000	-2.733056000	H	1.720546000	-1.327050000	7.572348000
C	0.412240000	-1.968614000	0.111400000	O	-0.698303000	-1.435187000	-4.758354000	H	1.293627000	-2.274526000	6.120836000
C	1.406225000	0.606719000	1.206100000	O	1.386911000	-0.207515000	5.921625000	H	0.026121000	-1.369766000	7.002208000
C	2.808605000	0.309855000	1.118853000	O	-1.386922000	0.207490000	5.921613000	H	-1.720581000	1.326992000	7.572353000
C	3.515110000	-0.028817000	2.324164000	H	-3.403343000	0.324278000	4.434253000	H	-1.293650000	2.274497000	6.120863000
C	2.867988000	-0.132759000	3.512026000	H	-4.587387000	0.188099000	2.263640000	H	-0.026149000	1.369727000	7.002232000
C	0.764288000	1.215350000	0.044009000	H	-4.414212000	0.148965000	-0.250008000				
C	1.373435000	1.030314000	-1.220674000	H	1.004884000	-2.423216000	-3.215063000				

S12. References

1. Kim, H.-J.; Lee, E.; Park, H.-s.; Lee, M. *J. Am. Chem. Soc.* **2007**, 129, (36), 10994-10995.
2. Saal, F.; Zhang, F.; Holzapfel, M.; Stolte, M.; Michail, E.; Moos, M.; Schmiedel, A.; Krause, A. M.; Lambert, C.; Würthner, F.; Ravat, P. *J. Am. Chem. Soc.* **2020**, 142, (51), 21298-21303.
3. Mallory, F. B.; Mallory, C. W., Photocyclization of Stilbenes and Related Molecules. In *Organic Reactions*, ed.; John Wiley & Sons, Inc.: 2005; pp 1–456; Mallory, F. B.; Mallory, C. W. *J. Org. Chem.* **1983**, 48, (4), 526–532.
4. Sillen, A.; Engelborghs, Y. *Photochem. Photobiol.* **1998**, 67, (5), 475-486.
5. Mataga, N.; Kaifu, Y.; Koizumi, M. *Bull. Chem. Soc. Jpn.* **1956**, 29, (4), 465-470; Grabowski, Z. R.; Rotkiewicz, K.; Rettig, W. *Chem. Rev.* **2003**, 103, (10), 3899-4032.
6. Frisch, M. J.; Trucks, G. W.; Schlegel, H. B.; Scuseria, G. E.; Robb, M. A.; Cheeseman, J. R.; Scalmani, G.; Barone, V.; Petersson, G. A.; Nakatsuji, H.; Li, X.; Caricato, M.; Marenich, A. V.; Bloino, J.; Janesko, B. G.; Gomperts, R.; Mennucci, B.; Hratchian, H. P.; Ortiz, J. V.; Izmaylov, A. F.; Sonnenberg, J. L.; Williams; Ding, F.; Lipparini, F.; Egidi, F.; Goings, J.; Peng, B.; Petrone, A.; Henderson, T.; Ranasinghe, D.; Zakrzewski, V. G.; Gao, J.; Rega, N.; Zheng, G.; Liang, W.; Hada, M.; Ehara, M.; Toyota, K.; Fukuda, R.; Hasegawa, J.; Ishida, M.; Nakajima, T.; Honda, Y.; Kitao, O.; Nakai, H.; Vreven, T.; Throssell, K.; Montgomery Jr., J. A.; Peralta, J. E.; Ogliaro, F.; Bearpark, M. J.; Heyd, J. J.; Brothers, E. N.; Kudin, K. N.; Staroverov, V. N.; Keith, T. A.; Kobayashi, R.; Normand, J.; Raghavachari, K.; Rendell, A. P.; Burant, J. C.; Iyengar, S. S.; Tomasi, J.; Cossi, M.; Millam, J. M.; Klene, M.; Adamo, C.; Cammi, R.; Ochterski, J. W.; Martin, R. L.; Morokuma, K.; Farkas, O.; Foresman, J. B.; Fox, D. J. *Gaussian 16 Rev. C.01*, Wallingford, CT, 2016.
7. Bruhn, T.; Schaumlöffel, A.; Hemberger, Y.; Bringmann, G. *Chirality* **2013**, 25, (4), 243-249.
8. Hanwell, M. D.; Curtis, D. E.; Lonie, D. C.; Vandermeersch, T.; Zurek, E.; Hutchison, G. R. *Journal of cheminformatics* **2012**, 4, (1), 1-17.
9. Heckmann, A.; Lambert, C. *Angew. Chem. Int. Ed.* **2012**, 51, (2), 326-392; Renz, M.; Theilacker, K.; Lambert, C.; Kaupp, M. *J. Am. Chem. Soc.* **2009**, 131, (44), 16292-16302.